

## RESEARCH PAPER

# Effects of non-euphoric plant cannabinoids on muscle quality and performance of dystrophic mdx mice

**Correspondence** Vincenzo Di Marzo and Fabio Arturo Iannotti, Endocannabinoid Research Group, Institute of Biomolecular Chemistry (ICB), National Research Council (CNR), Pozzuoli (NA) 80078, Italy. E-mail: vdimarzo@icb.cnr.it; fabio.iannotti@icb.cnr.it

**Received** 8 April 2018; **Revised** 8 July 2018; **Accepted** 12 July 2018

Fabio Arturo Iannotti<sup>1,\*</sup> , Ester Pagano<sup>2,\*</sup>, Aniello Schiano Moriello<sup>1</sup>, Filomena Grazia Alvino<sup>3</sup>, Nicolina Cristina Sorrentino<sup>3</sup>, Luca D'Orsi<sup>3</sup>, Elisabetta Gazzero<sup>4</sup>, Raffaele Capasso<sup>5</sup>, Elvira De Leonibus<sup>3,6</sup>, Luciano De Petrocellis<sup>1</sup> and Vincenzo Di Marzo<sup>1</sup> 

<sup>1</sup>Endocannabinoid Research Group, Institute of Biomolecular Chemistry (ICB), National Research Council (CNR), Pozzuoli (NA), Italy, <sup>2</sup>Department of Pharmacy, School of Medicine and Surgery, University of Naples Federico II, Naples, Italy, <sup>3</sup>Telethon Institute of Genetics and Medicine (TIGEM), Pozzuoli, Italy, <sup>4</sup>Gaslini Children's Hospital, Genoa, Italy, <sup>5</sup>Department of Agricultural Sciences, University of Naples Federico II, Naples, Italy, and <sup>6</sup>Institute of Genetics and Biophysics (IGB), National Research Council, Naples, Italy

\*The authors contributed equally.

### BACKGROUND AND PURPOSE

Duchenne muscular dystrophy (DMD), caused by dystrophin deficiency, results in chronic inflammation and irreversible skeletal muscle degeneration. Moreover, the associated impairment of autophagy greatly contributes to the aggravation of muscle damage. We explored the possibility of using non-euphoric compounds present in *Cannabis sativa*, cannabidiol (CBD), cannabidivarin (CBDV) and tetrahydrocannabidivarin (THCV), to reduce inflammation, restore functional autophagy and positively enhance muscle function *in vivo*.

### EXPERIMENTAL APPROACH

Using quantitative PCR, western blots and  $[Ca^{2+}]_i$  measurements, we explored the effects of CBD and CBDV on the differentiation of both murine and human skeletal muscle cells as well as their potential interaction with TRP channels. Male dystrophic mdx mice were injected i.p. with CBD or CBDV at different stages of the disease. After treatment, locomotor tests and biochemical analyses were used to evaluate their effects on inflammation and autophagy.

### KEY RESULTS

CBD and CBDV promoted the differentiation of murine C2C12 myoblast cells into myotubes by increasing  $[Ca^{2+}]_i$  mostly *via* TRPV1 activation, an effect that undergoes rapid desensitization. In primary satellite cells and myoblasts isolated from healthy and/or DMD donors, not only CBD and CBDV but also THCV promoted myotube formation, in this case, mostly *via* TRPA1 activation. In mdx mice, CBD (60 mg·kg<sup>-1</sup>) and CBDV (60 mg·kg<sup>-1</sup>) prevented the loss of locomotor activity, reduced inflammation and restored autophagy.

### CONCLUSION AND IMPLICATIONS

We provide new insights into plant cannabinoid interactions with TRP channels in skeletal muscle, highlighting a potential opportunity for novel co-adjuvant therapies to prevent muscle degeneration in DMD patients.

### LINKED ARTICLES

This article is part of a themed section on 8<sup>th</sup> European Workshop on Cannabinoid Research. To view the other articles in this section visit <http://onlinelibrary.wiley.com/doi/10.1111/bph.v176.10/issuetoc>

## Abbreviations

[Ca<sup>2+</sup>]<sub>i</sub>, intracellular calcium concentration; CBD, cannabidiol; CBDA, cannabidiolic acid; CBDV, cannabidivarin; CBG, cannabigerol; DM, differentiation media; DMD, Duchenne muscular dystrophy; GM, growth medium; IRTX, 5'-iodoresiniferatoxin; MyHC, myosin heavy chain; qPCR, quantitative PCR; THC, Δ<sup>9</sup>-tetrahydrocannabinol; THCV, Δ<sup>9</sup>-tetrahydrocannabivarin; Tnnt-1, troponinT-1; TRP channel, transient receptor potential channel

## Introduction

Skeletal muscle dystrophies encompass a large heterogeneous group of hereditary disorders associated with progressive and irreversible damage to muscle tissues. Among these disorders, Duchenne's muscular dystrophy (DMD) represents the most frequent form affecting about 1 in 3500 newborn baby boys (Govoni *et al.*, 2013). This disease is caused by deletions (65.8%), duplications (13.6%) and point mutations (20.6%) (Magri *et al.*, 2011) in the X-linked gene encoding for the structural protein dystrophin. In healthy mammalian skeletal and cardiac muscles, dystrophin plays a key structural role by physically coupling the sarcolemma cytoskeleton with the extracellular matrix. Therefore, the lack of functional dystrophin inevitably compromises the structure of the sarcolemma membrane, thus causing progressive muscle damage and failure (Matsumura *et al.*, 1993). The inflammatory response, activation of necrosis and exhaustion of regeneration cycles of muscle fibres are all known mechanisms leading to the exacerbation of the disease (Cruz-Guzmán *et al.*, 2015; Miyatake *et al.*, 2016).

There is also evidence that the lack of dystrophin impairs the polarity and self-renewal capacity of satellite cells, which are normally assigned to replace injured muscle fibres (Dumont *et al.*, 2015; Chang *et al.*, 2016). Thus, while, at the early stage of DMD, satellite cell-mediated muscle regeneration is able to attenuate degeneration (Duddy *et al.*, 2015), at later stages of disease progression this process is inefficient. In addition to the lack of dystrophin, the progressive decline in the autophagy process has been recently highlighted as one of the main causes of the inefficient function of satellite cells during DMD progression (Fiacco *et al.*, 2016). These results, in agreement with previous findings, suggested that autophagy represents a promising target for the treatment of DMD (Sandri *et al.*, 2013; De Palma *et al.*, 2014; Fiacco *et al.*, 2016).

Plant-derived cannabinoids (also known as phytocannabinoids) are a large group of compounds present in *Cannabis sativa*. Due to its euphoric properties, Δ<sup>9</sup>-tetrahydrocannabinol (THC) is the best known constituent of *Cannabis* (Di Marzo and Piscitelli, 2015). However, over 120 other phytocannabinoids have been reported in the literature (Morales *et al.*, 2017). Among them, cannabidiol (CBD) and its analogue cannabidivarin (CBDV), in contrast to Δ<sup>9</sup>-THC, do not induce euphoric effects and show efficacy, tolerability and safety in a considerable number of both preclinical and clinical studies (Burstein and Zurier, 2009; Hill *et al.*, 2012; Fernández-Ruiz *et al.*, 2013; Iannotti *et al.*, 2014a; Zurier and Burstein, 2016; Iffland and Grotenhermen, 2017). Besides CBD and CBDV, *C. sativa* may also contain high levels (up to 50%) of Δ<sup>9</sup>-tetrahydrocannabivarin (THCV), the propyl side chain analogue of THC (McPartland *et al.*, 2015; Fishedick, 2017). THCV is also undergoing clinical evaluation for the treatment of metabolic disorders (Jadoon *et al.*, 2016).

In this study we explored, for the first time, the potential use of CBD, CBDV and THCV as treatments of DMD on the basis of (i) the capability of these phytocannabinoids to directly or indirectly modulate, among others, the endocannabinoid signalling system (De Petrocellis *et al.*, 2011a,b) and (ii) the recently emerging role of the latter system in skeletal muscle differentiation (Iannotti *et al.*, 2014b). We measured the effects of these phytocannabinoids on murine myoblasts as well as on primary satellite cells and myoblasts isolated from healthy and DMD patients. For selected compounds, we also studied their effects on locomotor activity in a murine model of DMD (mdx mice). The **transient receptor potential (TRP)** superfamily of channels, as designated by International Union of Pharmacology (IUPHAR) (Alexander *et al.*, 2017b), exists in mammals as six families: TRPC, TRPM, TRPV, TRPA, TRPP and TRPML based on amino acid homologies. Since it is known that (i) TRPV, **TRPA1** and **TRPM8** cation channels are targets for these phytocannabinoids (Di Marzo and De Petrocellis, 2010; De Petrocellis *et al.*, 2011a,b; Hassan *et al.*, 2014; Iannotti *et al.*, 2014a) and (ii) TRP channels participate in the pathogenesis of DMD (Gailly, 2012; Ito *et al.*, 2013; Iwata *et al.*, 2013; Lorin *et al.*, 2015), we explored the functional interaction between phytocannabinoids and **TRPV1**, **TRPV2**, TRPA1 and TRPM8 channels in skeletal muscle cells.

## Methods

### Cell culture and reagents

Murine C2C12 myoblasts were propagated in a growth medium (GM) composed of DMEM (cat. n. 11995065; Life Technologies, Milan, Italy) supplemented with 10% FBS (cat. n. 16000044; Life Technologies), 5000 U·mL<sup>-1</sup> penicillin plus 5000 μg·mL<sup>-1</sup> streptomycin (cat. n. 15070063; Life Technologies) and 1% L-glutamine (cat. n. A2916801; Life Technologies). Proliferating C2C12 were induced to differentiate into myotubes by exposing them to differentiation medium (DM; DMEM; cat. n. 11995065; Life Technologies) supplemented with 0.1% FBS plus the addition of 5 μg·mL<sup>-1</sup> insulin and 5 μg·mL<sup>-1</sup> transferrin according to previously published protocols (Iannotti *et al.*, 2010).

Primary human satellite cells were provided by Innoprot (Bizkaia-Spain) and Sciencell (Carlsbad, CA, USA). Satellite cells were propagated in a GM recommended by Innoprot (Skeletal Muscle Cell Medium, cat. n. P60124). Myotube differentiation was achieved after exposure of satellite cells to a skeletal muscle cell DM provided by Applied Stem Cell (cat. n. ASE-5064, CA, USA).

Primary myoblasts were established from muscle biopsies of DMD donors after they had signed informed consent forms

and in accordance with the guidelines of the G. Gaslini Institute Ethical Committee and according to published procedures (Morosetti *et al.*, 2010). The myoblasts were propagated in Full Aneural Medium composed of DMEM (cat. n. 11995065) supplemented with 15% FBS, 20% Medium 199 (cat. n. 12350039), 1% insulin (cat. n. A11382II), 1% L-glutamine (cat. n. A2916801) and 15 000 U·mL<sup>-1</sup> penicillin plus 5000 µg·mL<sup>-1</sup> streptomycin (cat. n. 15070063), FGF (cat. n. PHG6015) and EGF (cat. n. PHG0311). All the reagents were provided by Life Technologies.

### RNA extraction and quantitative PCR

Total RNA isolation, purification and cDNA synthesis were performed as described previously (Iannotti *et al.*, 2010). Quantitative PCR (qPCR) was carried out in a real-time PCR system CFX384 (Bio-Rad) using the SsoAdvanced SYBR Green supermix (cat. n. 1725274, Bio-Rad Milan Italy) detection technique and specific primers are shown in Supporting Information Table S3. qPCR was performed on independent biological samples  $\geq 5$  for each experimental group. In addition, each sample was amplified simultaneously in quadruplicate in a one-assay run with a non-template control blank for each primer pair to control for contamination or primer-dimer formation, and the cycle threshold (Ct) value for each experimental group was determined. A housekeeping gene (the ribosomal protein S16) was used to normalize the Ct values, using the  $2^{-\Delta Ct}$  formula; differences in mRNA content between groups were expressed as  $2^{-\Delta\Delta Ct}$ , as previously described (Iannotti *et al.*, 2010).

### Confocal immunofluorescence analysis

C2C12 and/or primary human satellite cells were plated on poly (L-lysine)-coated coverslips in GM at a density of about 80% of confluency. The next day, the GM was replaced, and cells were exposed to DM plus vehicle (DMSO) or CBD, CBDV or THCv for 3 (C2C12) or 5 (satellite cells) days. After this time, cells were fixed in freshly made paraformaldehyde (4% wv<sup>-1</sup>) for 10 min. The cells were then incubated for 5 min with 0.1 M glycine, washed in cold PBS and incubated for 1 h with anti-mouse monoclonal anti-myosin heavy chain (MyHC) (dilution 1:500; Millipore, Vimodrone – Milan, Italy). Subsequently, the cells were incubated at room temperature for 1 h with a fluorescent secondary antibody (The Jackson Laboratory, Bar Harbor, ME, USA) anti-mouse IgG conjugated to CY3 (cat. n. 715-165-150) for anti-MyHC, diluted 1:200 in PBS containing 10% (v<sup>-1</sup>) FBS and 0.1% Triton X-100. DAPI was used as a nuclear marker. Coverslips were mounted in SlowFade (Life Technologies, Milan, Italy).

### Intracellular calcium measurement

The effects of CBD and CBDV in both C2C12 and satellite cells on intracellular Ca<sup>2+</sup> was determined by using Fluo-4 (Molecular Probes, Eugene, OR, USA). Briefly, cells were loaded for 1 h at room temperature with the methyl ester Fluo 4-AM 4 µM; containing 0.02% Pluoronic F-127 (Molecular Probes) in DMEM not containing FBS. Subsequently, cells were washed twice in Tyrode's buffer (145 mM NaCl, 2.5 mM KCl, 1.5 mM CaCl<sub>2</sub>, 1.2 mM MgCl<sub>2</sub>, 10 mM D-glucose and 10 mM HEPES, pH 7.4), resuspended in Tyrode's buffer and transferred to the quartz cuvette of the spectrofluorometer (Perkin-Elmer LS50B; Perkin-Elmer Life, Waltham, MA,

USA) under continuous stirring. Experiments were carried out by measuring cell-emitted fluorescence at 25°C (excitation  $\lambda = 488$  nm; emission  $\lambda = 516$  nm) before and after the addition of compounds. The effects of each phytocannabinoid was determined by normalizing its effect to the maximum Ca<sup>2+</sup> influx effect on intracellular calcium concentration ([Ca<sup>2+</sup>]<sub>i</sub>) observed after the application of 4 µM ionomycin (cat. n. I3909; Sigma Aldrich, Milan, Italy). The potency of palvanil, CBD, CBDV and THCv is reported as the concentration exerting half-maximal increases in [Ca<sup>2+</sup>]<sub>i</sub> (EC<sub>50</sub>). The TRPV1, TRPV2 and/or TRPA1 channel antagonists, **iodoresiniferatoxin (IRTX)**; 1 µM, **tranilast** (100 µM) and **AP18** (up to 50 µM), respectively, were added 5 min before the stimulation with phytocannabinoids.

*Cell transfection and gene silencing.* Satellite cells were plated in 60 mm culture dishes; the day after plating, cells were transfected with esiRNA human TRPA1 sequences (cat. n. EHU040601; Sigma Aldrich, MO, USA) using Lipofectamine RNAiMAX Transfection Reagent (cat. n. 13778030 Thermofisher, Milan, Italy), according to the manufacturer's instructions. After 48 h, satellite cells were used for qPCR and intracellular Ca<sup>2+</sup> functional assays.

*Animal care and use.* The experimental protocol was evaluated and approved by the Institutional Animal Ethics Committee for the use of experimental animals and conformed to guidelines for the safe use and care of experimental animals in accordance with the Italian D.L. no. 116 of 27 January 1992 and associated guidelines in the European Communities Council (86/609/ECC and 2010/63/UE). Animal studies are reported in compliance with the ARRIVE guidelines (Kilkenny *et al.*, 2010; McGrath and Lilley, 2015).

For this study, male wild-type (C57BL/10ScSnJ) and mdx (C57BL/10ScSn-DMDmdx/J) mice of 5 weeks of age weighing approximately 20–25 g were purchased from Charles River Laboratories (MI, Italy). This animal model was selected since it represents one of most used to study DMD (Collins and Morgan 2003; McGreevy *et al.*, 2015). All mice were housed in an individually ventilated cage system with a 12 h light–dark cycle (temperature 23 ± 2 °C, humidity 60%) and received standard mouse chow (Harlan Teklad) and water *ad libitum*. Control or mdx mice were injected i.p. (60 µL per animal) three times a week for 2 weeks with (i) vehicle (ethanol + Tween 20 + NaCl; 1:1:8), (ii) CBD (60 mg·kg<sup>-1</sup>) and (iii) CBDV (60 mg·kg<sup>-1</sup>). Animals were housed in groups of four to five; animals belonging to each cage were randomly assigned to the different experimental groups. The experimenter performing the behavioural testing was blind to the genotype and treatment.

### Locomotor tests

*Rotarod test.* The rotarod test was performed in control and dystrophic mice immediately before the beginning of the pharmacological treatment (5 and 32 weeks) and at the end of 2 weeks of treatment with vehicle, CBD or CBDV following published protocol with slight modifications (Aartsma-Rus and van Putten, 2014). In particular, we repeated the measurements three times, whereas the published protocol that this is based on conducted a maximum of two repeats.

**Muscle strength test.** To test the forelimb strength of mdx mice treated or not with the aforementioned compounds, four weights of 20, 33, 46 and 59 g constituted the apparatus. Procedures and the analysis of results were performed following published protocols (Deacon, 2013).

**Forelimb grip strength test.** Forelimb grip strength was measured using the grip strength metre (Ugo Basile, Italy). A force transducer attached to the instrument measures the maximum force applied by the animal on a grid during the pull. Animals were moved horizontally towards the grid and pulled away from it so that their grasp was broken. The maximal force applied in g measured from three trials of three pulls was recorded for each mouse. An intertrial interval of 45 min allowed the animals to recover. The mean value between pulls and between trials was measured and normalized for body weight.

**Histological analysis.** Once control and mdx mice were previously anaesthetized with 75% CO<sub>2</sub>/25% O<sub>2</sub>, skeletal muscle were quickly dissected and snapped ... Skeletal muscles were snapped frozen in liquid nitrogen-chilled isopentane. Seven-micrometre sections were cut from the frozen skeletal tissues, fixed and stained with Harris haematoxylin and eosin (H&E) for morphological analysis, following standard procedures. Sections were then examined using a Scan-Scope slide scanner (Leica scn400). The total number of centralized nuclei in the muscle fibres stained by H&E were calculated on 500–800 fibres by using an ImageJ programme in single blind by two pathologists.

**Western blotting analysis.** C2C12 cells were subjected to western blot analysis following the procedure previously described (Iannotti *et al.*, 2014b). To isolate total proteins from whole muscle, control (C57BL/10ScSnJ) or mdx (C57BL/10ScSn-DMDmdx/J) mice were anaesthetized with 75% CO<sub>2</sub>/25% O<sub>2</sub> and killed by cervical dislocation, and blood was collected by cardiac puncture (see ELISA technique for details). Gastrocnemius and diaphragms were quickly removed and kept on dry ice until the whole procedure was completed. Muscles from control and mdx mice were homogenized in lysis buffer composed of 150 mM NaCl, 1 mM EDTA, 1% (v/v<sup>-1</sup>) Triton X-100, 2.5 mM sodium pyrophosphate, 1 mM 2-glycerophosphate, 1 mM Na<sub>3</sub>VO<sub>4</sub>, 20 mM Tris-HCl pH 8.1 %SDS, plus protease inhibitor (cat. n. P8340, Sigma-Aldrich, MI, Italy) at pH 7.4. Lysates were kept in an orbital shaker incubator at 220 rpm at 4°C for 30 min and then centrifuged for 15 min at 13 000× g at 4°C. The supernatants were transferred to tubes and quantified by DC Protein Assay (Bio-Rad, Milan, Italy). Subsequently, the samples (60 µg of total protein) were heated at 70°C for 10 min in NuPAGE LDS Sample Buffer (cat. n. NP0007, Life Technologies) plus Sample Reducing Agent (cat. n. NP0004, Life Technologies) and loaded onto 4–12% Bis-Tris Protein Gels (cat. n. NP0336PK2, Life Technologies) and then transferred to a PVDF membrane. The primary antibodies used were as follows: (i) rabbit anti-Trpv1 (phospho S800) antibody (1:500; cat. n. PAB8499, Abnova, Tapei, Taiwan); (ii) rabbit anti-Trpv1 (total) antibody (cat. n. ACC-030, Alomone, Israel); and (iii) rabbit anti-LC3B antibody (1:1000; cat. n. 2775; Cell signalling,

Beverly, MA, USA). An anti-GAPDH antibody (1D4) (cat. n. NB300-221) (1:5000; Novus) was used to check for equal protein loading. Reactive bands were detected by chemiluminescence (ECL-plus; Bio-Rad, Segrate, Italy). The intensity of bands was analysed on a ChemiDoc station with Quantity-one software (Biorad, Segrate, Italy).

**ELISA assays.** Control and mdx mice treated with vehicle (1:1:8; ethanol + Tween 20 + NaCl<sub>2</sub>) or phytocannabinoids (CBD and CBDV) were anaesthetized with 75% CO<sub>2</sub>/25% O<sub>2</sub> and, subsequently, blood was withdrawn by cardiac puncture and collected into EDTA-treated tubes. Blood cells were then precipitated by centrifugation for 10 min at 1000–2000× g at 4°C. The supernatant (plasma) obtained was filtered and centrifuged in Amicon Ultra-0.5 mL Centrifugal Filters (Melk, MI, Italy) to concentrate the proteins with a molecular weight >10 KDa. The ELISA assay was performed by the use of either **TNFα** (cat. n. KHC3011, Life Technologies) or **IL-6** (cat. n. KMC0061, Life Technologies) following the manufacturer's instruction.

### Data analysis

The data and statistical analysis comply with the recommendations on experimental design and analysis in pharmacology (Curtis *et al.*, 2018). Data are expressed as means ± SEM of values and 'n' refers to the number of samples for each set of experiments. Statistical analysis was performed using the free demo version of Minitab and Prism 7.0 (GraphPad Software Inc., La Jolla, CA, USA). The Anderson-Darling test was used to determine if a data set conformed to a normal distribution. Once this information was obtained, a *t*-test and/or one-way ANOVA followed by Bonferroni's analysis was used to determine statistically significant differences between two or more independent biological groups. Statistically significant differences were accepted when *P* was < 0.05.

**Reagents.** All phytocannabinoids including CBD (CG-0801), CBDV (CG-1102), THCV (CG-1023), cannabigerol (CBG) (CG-0903) and cannabidiolic acid (CBDA) (CG-1104) were provided by GW Pharmaceuticals (Cambridge, UK).

### Nomenclature of targets and ligands

Key protein targets and ligands in this article are hyperlinked to corresponding entries in <http://www.guidetopharmacology.org>, the common portal for data from the IUPHAR/BPS Guide to PHARMACOLOGY (Harding *et al.*, 2018), and are permanently archived in the Concise Guide to PHARMACOLOGY 2017/18 (Alexander *et al.*, 2017a,b,c,d).

## Results

### Effect of acute or prolonged exposure to cannabinol, cannabidiarin and tetrahydrocannabivarin on differentiating murine C2C12 myoblasts

To explore the potential effects of plant cannabinoids (or phytocannabinoids) on skeletal muscle cells, we initially measured the effect of either acute or prolonged exposure to

CBD, CBDV, THCV, CBG and CBDA on differentiating C2C12 cells. For acute exposure, the phytocannabinoids were added to the DM for 5, 15 min or 3 h; afterwards, they were removed, and fresh DM was added for 72 h. In the case of prolonged exposure, C2C12 myoblasts were exposed to phytocannabinoids for up to 72 h (Iannotti *et al.*, 2010). Our results indicate that myoblasts exposed to CBD (1  $\mu$ M) and CBDV (1 and 3  $\mu$ M), compared to control (up to 0.003%, DMSO), show an increased mRNA expression of the two canonical skeletal muscle differentiation marker myogenin and troponinT-1. This effect was more prominent following acute (5, 15 min and 3 h) rather than prolonged (72 h) exposure [Figure 1A–D; myogenin ( $F_{(5, 29)} = 21.28$ ,  $P < 0.05$ ) and Tnnt-1 ( $F_{(5, 35)} = 29$ ,  $P < 0.05$ ) for CBD; myogenin ( $F_{(5, 36)} = 12.57$ ,  $P < 0.05$ ) and Tnnt-1 ( $F_{(5, 36)} = 41.25$ ,  $P < 0.05$ ) for CBDV]. The effect of prolonged

exposure to CBD (1  $\mu$ M) or CBDV (3  $\mu$ M) on differentiating C2C12 was confirmed by immunocytochemical analysis of the expression levels of myosin heavy chain (MyHC), a late marker of myotube formation (Iannotti *et al.*, 2010; Figure 1E,F).

Before selecting the concentrations of CBD and CBDV, we conducted preliminary experiments inducing C2C12 myoblasts to differentiate for 72 h in the presence of increasing concentrations (from 0.1 to 3  $\mu$ M) of each phytocannabinoid. The results indicated that concentrations lower than 1  $\mu$ M of both CBD and CBDV were ineffective (Supporting Information Figure S1), whereas CBD at 3  $\mu$ M inhibited myogenin expression levels (Supporting Information Figure S1). In addition, THCV at all concentrations tested did not produce significant effects. CBG and CBDA were also ineffective up to 1  $\mu$ M, and inhibited

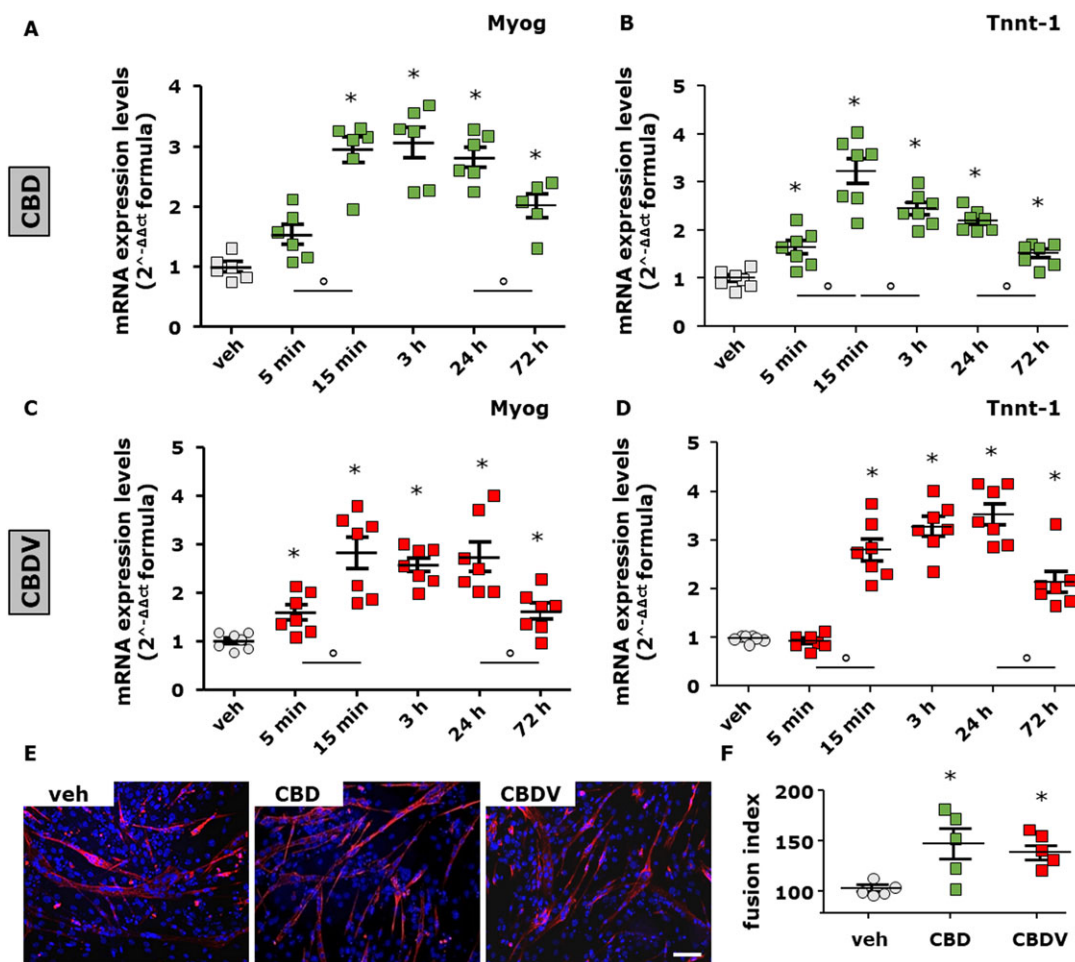


**Figure 1**

Measurement of skeletal muscle differentiation markers in C2C12 cells following short or prolonged exposure to CBD and CBDV. Transcript levels of myogenin (Myog) and Tnnt-1 in murine C2C12 cells exposed to DM following acute (5, 15 min and 3 h) or prolonged (24 or 72 h) exposure to CBD 1  $\mu$ M (A, B) or CBDV 1  $\mu$ M (C, D). The quantification of mRNA levels for myogenin and Tnnt-1 was performed by quantitative real-time PCR. Data represent the mean  $\pm$  SEM of six separate determinations. Data are expressed as  $2^{-\Delta\Delta Ct}$  relative to S16, as described in Methods. (E, F) Morphological analysis of myotube formation in C2C12 cells exposed to DM for 72 h in the presence of vehicle (DMSO  $\leq 1\%$ , control;  $n = 5$ ), CBD 1  $\mu$ M ( $n = 5$ ) or CBDV 3  $\mu$ M ( $n = 5$ ). MyHC (red) and DAPI (blue) (Scale bar, 10  $\mu$ m). The fusion index was calculated in both vehicle- and CBD- or CBDV-treated cells. Data sets were compared by use of one-way ANOVA followed by Bonferroni's test. Differences were considered statistically significant when  $P$  was  $\leq 0.05$ . The asterisk (\*) denotes a  $P$  value of  $\leq 0.05$  versus vehicle (DMSO) control group.

myogenin expression levels at higher concentrations (data not shown).

Based on these results, CBD and CBDV were the only two phytocannabinoids selected for all our subsequent experiments conducted in murine cells.

### Expression profile and pharmacological role of TRP channels

We measured mRNA expression levels of TRPV1–6 as well as of TRPA1 and TRPM8 in both myoblasts and myotubes of C2C12 cells by use of qPCR. We found that, with the exception of TRPV1 and TRPV2, the TRP channels analysed were barely or not at all expressed (Supporting Information Table S1A).

In order to unmask the potential involvement of TRPV1 and TRPV2 in CBD and CBDV effects on myotube formation, we induced C2C12 myoblasts to differentiate for 72 h in the presence of increasing concentrations of two agonists of the two channels, palvanil and **probenecid** respectively (De Petrocellis *et al.*, 2011a; Robbins *et al.*, 2012). In addition, we measured the effects of increasing concentrations of antagonists such as IRTX (for TRPV1) or tranilast (for TRPV2) (Nie *et al.*, 1997; Seabrook *et al.*, 2002).

As shown in Supporting Information Figure S2, palvanil at low concentrations (0.1–0.3  $\mu\text{M}$ ) enhanced the expression of myogenin and Tnnt-1 mRNA (Supporting Information Figure S2A,B), whereas at higher concentrations (1–3  $\mu\text{M}$ ), an opposite effect was observed (Supporting Information Figure S2A, B;  $F_{(5, 36)} = 12.95$ ,  $P < 0.05$  for myogenin;  $F_{(5, 34)} = 43.53$ ,  $P < 0.05$  for Tnnt-1). However, IRTX, at 1 and 3  $\mu\text{M}$ , inhibited the expression of myogenin (Supporting Information Figure S2C;  $F_{(5, 35)} = 19.26$ ,  $P < 0.05$ ) and Tnnt-1 (Supporting Information Figure S2D;  $F_{(5, 35)} = 15.11$ ,  $P < 0.05$ ). In contrast, the non-selective TRPV2 agonist probenecid or antagonist tranilast did not produce significant effects on myogenin expression (Supporting Information Figure S2E,F).

### CBD and CBDV increase $[\text{Ca}^{2+}]_i$ and promote C2C12 cell differentiation in a manner dependent on TRPV1 activation

As a transient increase in intracellular  $\text{Ca}^{2+}$  is known to represent one of the first events triggering myoblast differentiation (Cooper, 2001), we explored whether differentiation of C2C12 myoblasts by TRPV agonists could be dependent on an increase in  $[\text{Ca}^{2+}]_i$ . Although measuring such transient

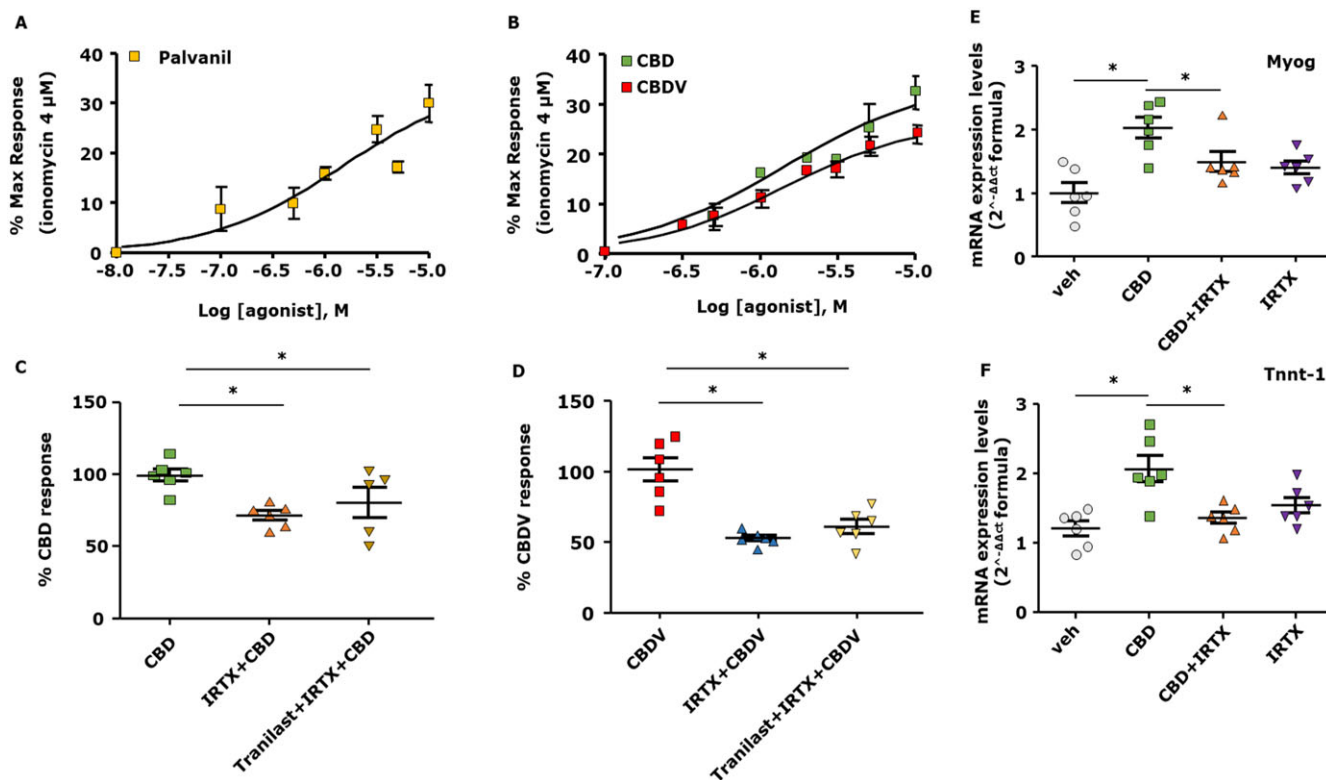


**Figure 2**

CBD and CBDV increase the concentration of intracellular  $\text{Ca}^{2+}$  levels and promote the differentiation in C2C12 cells in a TRPV1, but not TRPV2, dependent manner. Concentration–response curve showing the effect of palvanil (A) and CBD or CBDV (B) in C2C12 cells. (C, D) Effect of CBD 3  $\mu\text{M}$  or CBDV 3  $\mu\text{M}$  evaluated in the presence of IRTX 0.6  $\mu\text{M}$  (a selective TRPV1 antagonist) or tranilast 100  $\mu\text{M}$  (a non-selective TRPV2 antagonist) used alone or in combination. (E, F) mRNA expression levels of myogenin (Myog) and Tnnt-1 in C2C12 cells exposed to DM in the presence of CBD (1  $\mu\text{M}$ ) plus IRTX (0.6  $\mu\text{M}$ ). Data represent the mean  $\pm$  SEM of six separate determinations. Data sets were compared by use of one-way ANOVA followed by Bonferroni's test. Differences were considered statistically significant when \* $P$  was  $\leq 0.05$ .

increases in cells suspended in a cuvette while being stirred is not reflective of physiological conditions, we have used this method as it has been employed in several studies in our and other laboratories, with results that have in most cases been confirmed in more physiologically relevant settings (Robinson *et al.*, 2004; De Petrocellis *et al.*, 2011b; Pan *et al.*, 2012; Patel *et al.*, 2013).

Stimulation with palvanil led to an increase in  $[Ca^{2+}]_i$  in a concentration-dependent manner (Figure 2A), as was the case with CBD and CBDV (Figure 2B). C2C12 myoblasts were pre-incubated for 15 min with IRTX (0.6  $\mu$ M) or tranilast (100  $\mu$ M), before exposure to CBD (3  $\mu$ M) or CBDV (3  $\mu$ M). As shown in Figure 2C,D, in the absence of TRPV1 and TRPV2 antagonists, CBD or CBDV caused a significant elevation of  $[Ca^{2+}]_i$ , whereas in the presence of IRTX, CBD and CBDV effects were significantly, although not fully, inhibited (Figure 2C,D). Notably, the inhibitory effect of IRTX was not further increased in the presence of tranilast (Figure 2C,D). Importantly, the promotion of myogenin and Tnnt-1 expression by CBD was significantly reduced in the presence of IRTX [Figure 2E,F; myogenin ( $t = 5.98$  d.f. = 8) and Tnnt-1 ( $t = 3.43$ , d.f. = 10)]. In summary, these results seem to indicate that the effects of CBD and CBDV in C2C12 myoblasts are, at least in part, dependent on the activation of TRPV1, rather than TRPV2, channels.

### Functional activation and desensitization of TRPV1 by palvanil in C2C12 cells

In a manner similar to CBD and CBDV, we found that in differentiating myoblasts, palvanil (1  $\mu$ M) increased the mRNA expression levels of both myogenin ( $F_{(3, 23)} = 30.81$ ,  $P < 0.05$ ) and Tnnt-1 ( $F_{(3, 24)} = 43.53$ ,  $P < 0.05$ ) in a more prominent manner following acute (5 and 15 min) compared to prolonged (48 h) exposure (Figure 3A,B).

Several studies have demonstrated that activation of protein kinases causes phosphorylation of TRPV1 that leads to its increased sensitivity (Cortright and Szallasi, 2004; Jendryke *et al.*, 2016). Prolonged exposure to agonists causes dephosphorylation, inactivating the channels and rendering them refractory to further stimulation (Mohapatra and Nau, 2005; Vyklický *et al.*, 2008). Therefore, we searched for potential changes in the phosphorylation state of TRPV1 in C2C12 cells following their exposure to palvanil. Using a selective antibody directed against the region of Ser<sup>800</sup> of TRPV1 (Iannotti *et al.*, 2014a), we found that after 48 h exposure to 3  $\mu$ M palvanil, phosphorylation at that site was significantly reduced, suggestive of its desensitization (Figure 3C,D). The antagonist IRTX did not lead to a reduction in phosphorylation (Figure 3C,D). Palvanil at 0.3  $\mu$ M did not lead to a change in the phosphorylation state of TRPV1 (Supporting Information Figure S3). In conclusion, these results may provide an explanation for the opposite effects found here between the

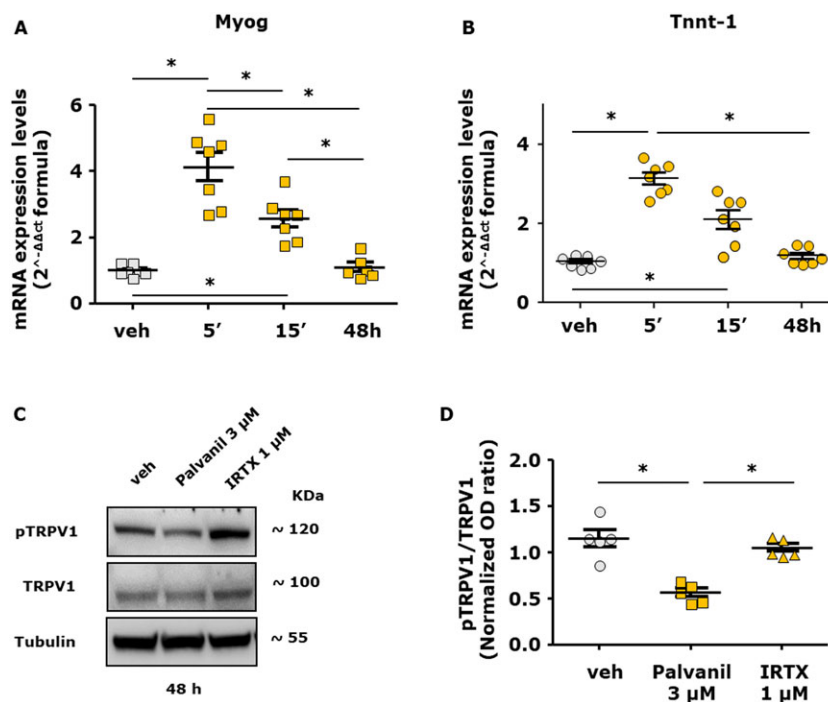


### Figure 3

Effect of short or prolonged stimulation with palvanil in C2C12 cells. (A, B) Quantification of transcripts levels of myogenin (Myog) and Tnnt-1, evaluated by quantitative real-time PCR, in C2C12 cells induced to differentiate in DM following the acute (5 and 15 min) or prolonged (48 h) exposure to palvanil 1  $\mu$ M. (C) Representative blot showing the chemiluminescent signal generated by the anti-phosphoTRPV1 antibody (at the phosphorylation site Ser<sup>800</sup> of TRPV1) evaluated by western blot analysis in C2C12 cells exposed for 48 h to DM in the presence of palvanil (3  $\mu$ M) or IRTX (1  $\mu$ M). (D) The graph shows the quantification of pTRPV1 signal (OD) normalized to the OD of TRPV1. Data represent the mean  $\pm$  SEM of five separate determinations. Data sets were compared by use of one-way ANOVA followed by Bonferroni's test. Differences were considered statistically significant when  $*P$  was  $\leq 0.05$ .

lowest (0.1 and 0.3  $\mu\text{M}$ ) and highest (1 and 3  $\mu\text{M}$ ) concentrations of palvanil and suggest that prolonged exposure to CBD and CBDV can induce desensitization of TRPV1 in differentiating C2C12 cells.

### Effect of CBD and CBDV on differentiating primary human myoblasts isolated from DMD donors

In order to explore the use of phytocannabinoids in human skeletal muscle cells, we isolated primary myoblasts from seven different donors (ranging from 1 to 7 years old) diagnosed with DMD caused by different mutations in the dystrophin gene (see Supporting Information Table S2). Proliferating myoblasts at a confluence of about 80–90% were exposed to CBD (1  $\mu\text{M}$ ) or CBDV (3  $\mu\text{M}$ ) in DM for 4 days. We found that CBD and CBDV promoted the expression of Tnnt-1 and myogenin in differentiating myoblasts isolated from patients D2 to D7, whereas those from patient D1 showed only Tnnt-1, but not myogenin, increased expression and, in those from patient D6, the opposite result was found (Figure 4A,B). Importantly, by combining the results from

all patients, we observed a significant difference in the expression levels of myogenin and Tnnt-1 between vehicle (DMSO) and and phytocannabinoid-treated myoblasts (Figure 4C,D).

### CBD, CBDV and THCv enhance primary human satellite cell differentiation

As mentioned above, THCv was not effective in murine myoblasts. However, since we recently demonstrated that antagonists of the cannabinoid type 1 (**CB<sub>1</sub>**) receptor promote murine as well as human myoblast and satellite cell differentiation *in vitro* (Iannotti *et al.*, 2014b) and that this compound shows antagonist activity at CB<sub>1</sub> receptors *in vitro* (McPartland *et al.*, 2015), we tested its effect together with CBD and CBDV in human satellite cells. Thus, primary satellite cells from healthy donors were induced to differentiate for 5 days in the presence of CBD (1  $\mu\text{M}$ ), CBDV (3  $\mu\text{M}$ ) or THCv (3  $\mu\text{M}$ ). As shown in Figure 5A, we found that the transcript levels of myogenin, Tnnt-1 and MyHC were significantly higher than those detected in cells treated with vehicle. These effects were confirmed by confocal immunofluorescence analysis that revealed the induction of MyHC

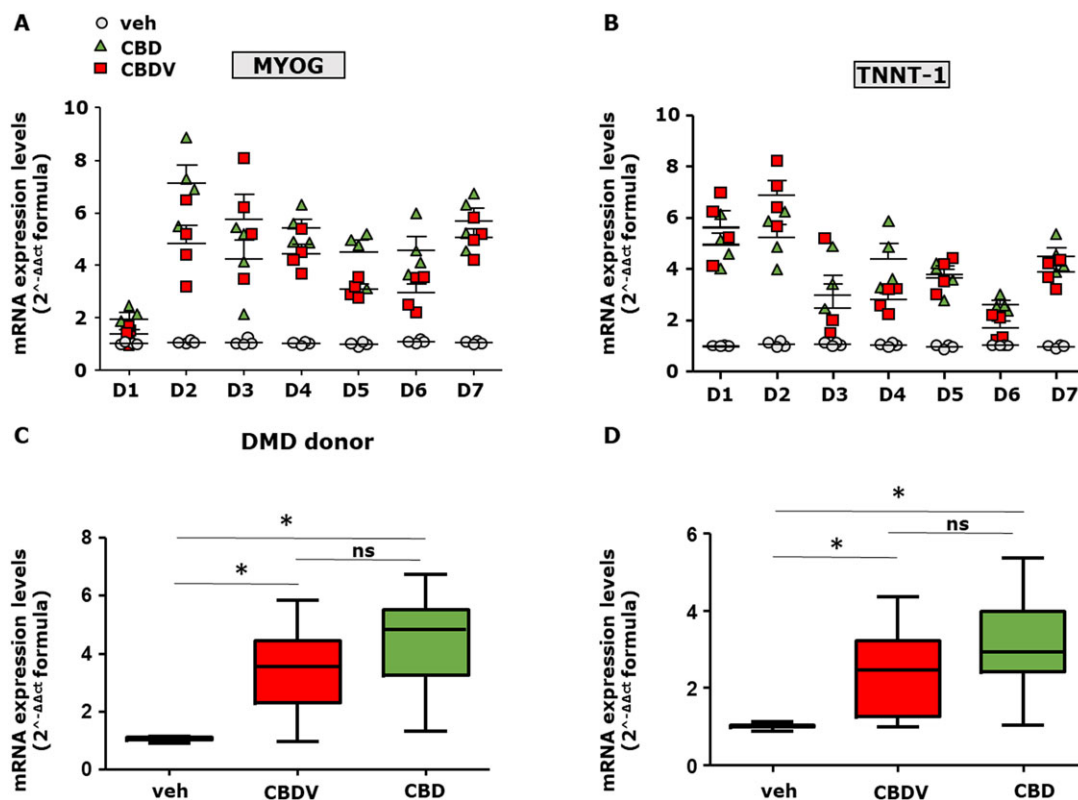


**Figure 4**

Effect of CBD and CBDV in differentiating myoblasts isolated from DMD donors. (A, B) Grouped column scatter plot showing the mRNA expression levels of MYOG and TNNT-1 in primary human myoblasts isolated from DMD patients and induced to differentiate in the presence of vehicle (0.001% DMSO), CBD (1  $\mu\text{M}$ ) or CBDV (3  $\mu\text{M}$ ). The quantification of transcripts was performed by quantitative real-time PCR. (C, D) The graphs show the differences in the expression level of MYOG and TNNT-1 between vehicle and CBD (1  $\mu\text{M}$ ) or CBDV (3  $\mu\text{M}$ ) treated myoblasts, calculated by combining the DMD patient's results together. Data are expressed as 2<sup>-ΔΔct</sup> formula relative to S16, as described in Methods. Data represent the mean ± SEM from the seven patients, repeated in quadruplicate. Data sets were compared by one-way ANOVA followed by Bonferroni's test. Differences were considered statistically significant when \**P* was ≤ 0.05.



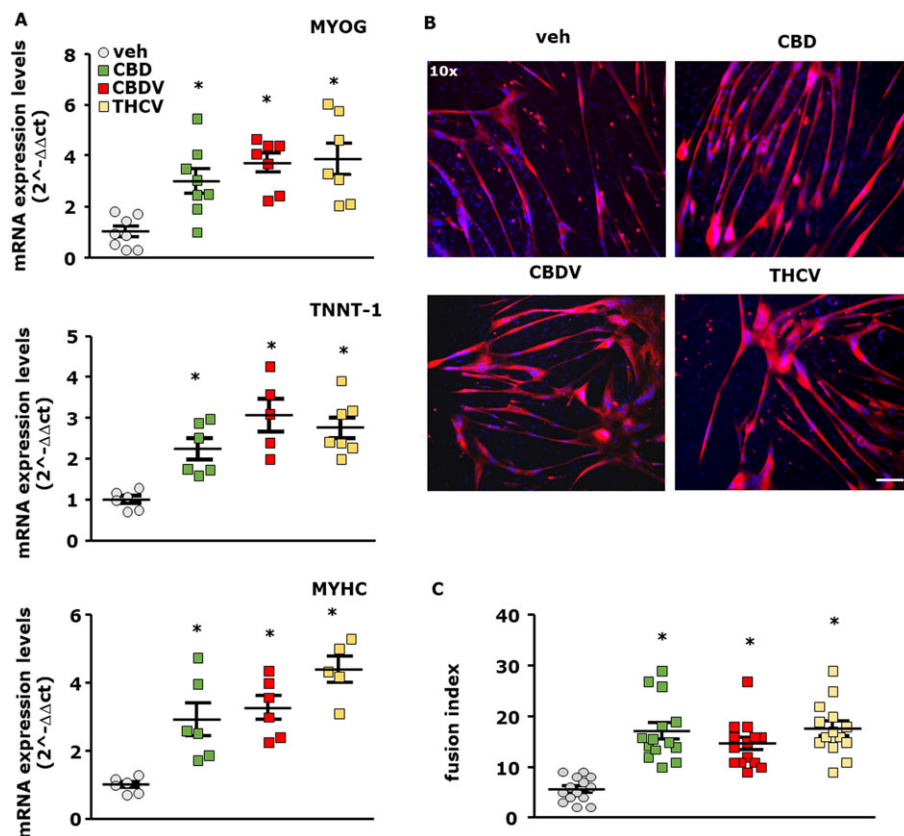


**Figure 5**

Effect of CBD, CBDV and THCv in differentiating primary human satellite cells. (A) Transcript levels of myogenin (MYOG), TNNT-1 and MyHC in human satellite cells exposed to DM in the presence of CBD 1  $\mu$ M, CBDV 3  $\mu$ M and THCv 3  $\mu$ M for 5 days. The quantification of transcripts for MYOG and TNNT-1 was performed by quantitative real-time PCR. Data represent the mean  $\pm$  SEM of  $n \geq 5$  determinations. Data are expressed as  $2^{-\Delta\Delta ct}$  relative to S16, as described in Methods. (B) Morphological analysis of myotube formation in satellite cells exposed to DM for 5 days in the presence of vehicle (0.003% DMSO, control;  $n = 14$ ), CBD 1  $\mu$ M ( $n = 14$ ), CBDV 3  $\mu$ M ( $n = 14$ ) or THCv 3  $\mu$ M ( $n = 14$ ). MyHC (red) and DAPI (blue) (Scale bar, 10  $\mu$ m). The fusion index was calculated in vehicle and CBD-, CBDV- or THCv-treated cells. Data sets were compared by use of one-way ANOVA followed by Bonferroni's test. Differences were considered statistically significant when  $*P$  was  $\leq 0.05$ .

expression (Figure 5B). Staining with DAPI confirmed *in vitro* myotube formation, as multiple nuclei were evident in single fibres (Figure 5B).

### TRP channel expression profile in primary human satellite cells

Although we demonstrated that in C2C12 cells TRPV1 and TRPV2 channels were most highly expressed, qPCR analysis revealed that, in human satellite cells, among all the TRP channels investigated, the TRPA1 gene exhibited the highest degree of expression (Supporting Information Table S1B).

### CBD, CBDV and THCv increase $[Ca^{2+}]_i$ levels and promote differentiation in human satellite cells via TRPA1 channel activation

In the light of the results described above, we tested whether the pro-differentiation effect exerted by CBD, CBDV and THCv could be attributed to their interaction with TRP channels. This was achieved using the same experimental approach described before for C2C12 cells, that is, we first measured intracellular  $Ca^{2+}$  following satellite cell exposure

to CBD, CBDV or THCv in the presence or absence of TRPV1, TRPV2 or TRPA1 antagonists. As shown in Figure 6A–C, stimulation of satellite cells with CBD, CBDV or THCv increased the  $[Ca^{2+}]_i$  in a concentration-dependent manner. As shown in Figure 6D–F, in the presence of IRTX (1  $\mu$ M) or tranelast (100  $\mu$ M), the effects of CBD, CBDV or THCv were unchanged, whereas in the presence of AP18 20 and 50  $\mu$ M, a selective antagonist of TRPA1 (Okubo *et al.*, 2012), the effects of CBDV and THCv were significantly reduced (Figure 6E,F). In contrast, the effect of CBD was less reduced by AP18 (Figure 6D). As further evidence that CBDV and THCv act by activating TRPA1 in satellite cells, we targeted the mRNA products of the TRPA1 gene by transfecting selective siRNA sequences into the cells. After 48 h, TRPA1-silenced satellite cells were used to measure  $[Ca^{2+}]_i$  or induced to differentiate following stimulation with CBDV or THCv. As shown in Supporting Information Figure S4A, following the stimulation with CBDV or THCv 3  $\mu$ M, the calcium signal induced by the two compounds in TRPA1-silenced satellite cells was significantly lower than that in cells transfected with scrambled sequences. In addition, in differentiating TRPA1-silenced satellite cells, which showed slightly reduced expression levels of myogenin as compared to

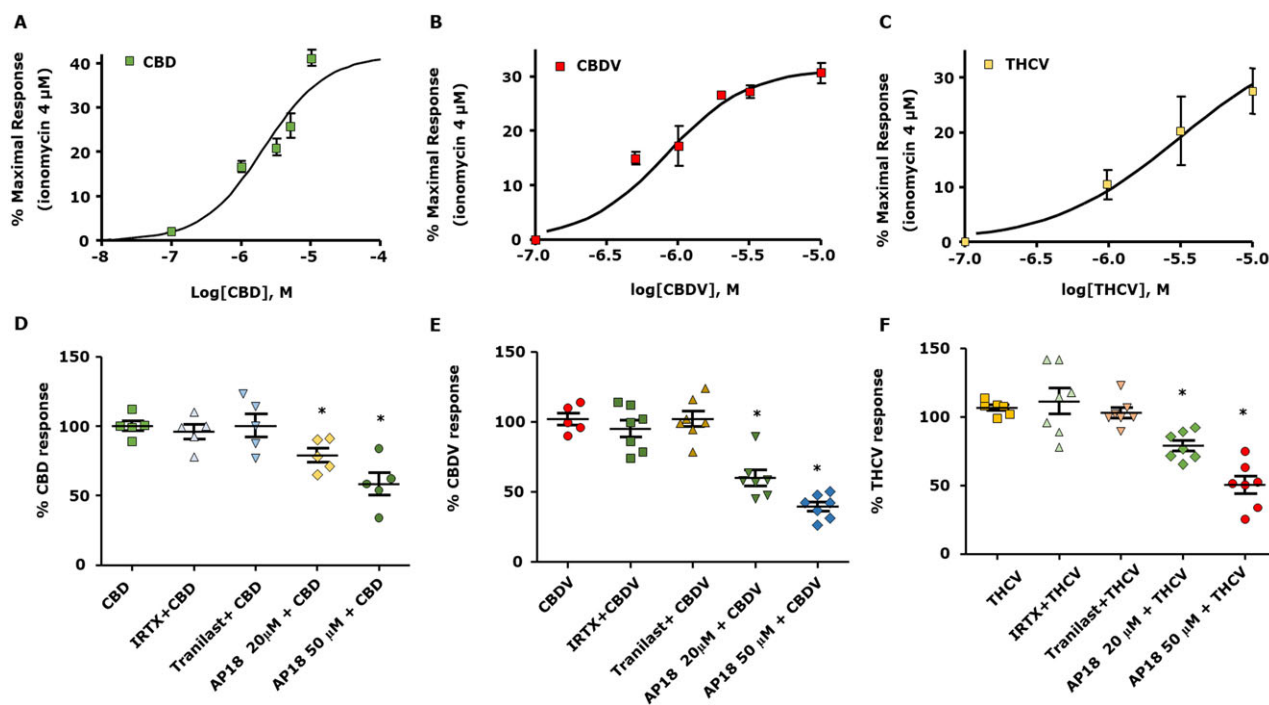


**Figure 6**

Effect of CBD, CBDV and THCv on intracellular Ca<sup>2+</sup> levels in the presence or absence of TRPV1, TRPV2 and TRPA1 antagonists in human satellite cells. Concentration–response curves showing the effect of CBD (A), CBDV (B) and THCv (C) on satellite cells. (D, F) Effect of CBD 3 μM, CBDV 3 μM and THCv 3 μM measured in the presence of IRTX 0.6 μM, a TRPV1 antagonist, 100 μM tranilast, a non-selective TRPV2 antagonist, or 20 and 50 μM of AP18, a selective TRPA1 antagonist. Data represent the mean ± SEM of ≥5 determinations. Data sets were compared by use of one-way ANOVA followed by Bonferroni's test. Differences were considered statistically significant when \**P* ≤ 0.05.

scramble sequence-transfected cells, the differentiating effect of CBDV and THCv was completely prevented (Supporting Information Figure S4B). These results suggest that CBDV and THCv, but less so CBD, elevate intracellular Ca<sup>2+</sup> and promote the differentiation of human satellite cells in a manner dependent on the activation of TRPA1 channels.

### Effect of CBD and CBDV on muscle activity in dystrophic mice

The above results show that of all the phytocannabinoids tested, CBD and CBDV had differentiating activity in both murine and human skeletal muscle cells. In order to gain information about the effects of CBD and CBDV *in vivo*, we evaluated these compounds in a widely used murine model of DMD. With this aim, we used mdx mice, a widely used animal model of DMD (Collins and Morgan, 2003; McGreevy *et al.*, 2015). These were treated with CBD or CBDV at 20, 40 and 60 mg·kg<sup>-1</sup>. We found that the only dose producing significant effects was 60 mg·kg<sup>-1</sup> for both compounds.

Male mdx mice of 5 weeks of age, the period of disease onset, were randomly divided into groups receiving (i) vehicle to serve as control, (ii) CBD (60 mg·kg<sup>-1</sup>), and (iii) CBDV (60 mg·kg<sup>-1</sup>). Compounds were injected *i.p.* three times a week from weeks 5 to 7 of age.

Following treatment, mice were subjected to a rotarod and weight tests according to published procedures (Deacon,

2013; Aartsma-Rus and van Putten, 2014). Locomotor activity at week 5, when compared to control mice, was not changed, but time spent on the rod significantly declined by week 7 (Figure 7A). Locomotor activity of control mice was not changed in any of the test periods (Figure 7, grey squares). At 7 weeks, mdx mice treated with CBD (60 mg·kg<sup>-1</sup>) or CBDV (60 mg·kg<sup>-1</sup>) spent a significantly longer time on the rotarod compared to the mdx vehicle-treated mice, to an extent that was similar to that of wild-type mice (Figure 7A, right; *F*<sub>(4, 69)</sub> = 8.728, *P* < 0.05).

In the weight and forelimb grip strength test, we found that 5-week-old mdx mice showed significantly reduced muscle strength compared to wild-type littermates (Figure 7B,C, left); strength was further reduced until 7 weeks of age (Figure 7B,C, right). Similar to the rotarod test results, we found that treatment for 2 weeks with CBD (60 mg·kg<sup>-1</sup>) or CBDV (60 mg·kg<sup>-1</sup>) restored the loss of muscle strength (Figure 7B,C).

Furthermore, to evaluate the effect of these treatments in a more advanced state of the disease, the same experimental procedure was repeated from weeks 32 to 34. At 34 weeks, when the muscle damage had further progressed, we found that 2 weeks of treatment with CBD (60 mg·kg<sup>-1</sup>) or CBDV (60 mg·kg<sup>-1</sup>) led to full recovery of the locomotor activity in the rotarod (Figure 8A; *F*<sub>(4, 58)</sub> = 9.431, *P* < 0.05) and weight (Figure 8B; *F*<sub>(4, 49)</sub> = 5.242, *P* = 0.05) test.

H&E staining revealed that in the gastrocnemius muscle of 34-week-old mdx mice treated with vehicle (ethanol +

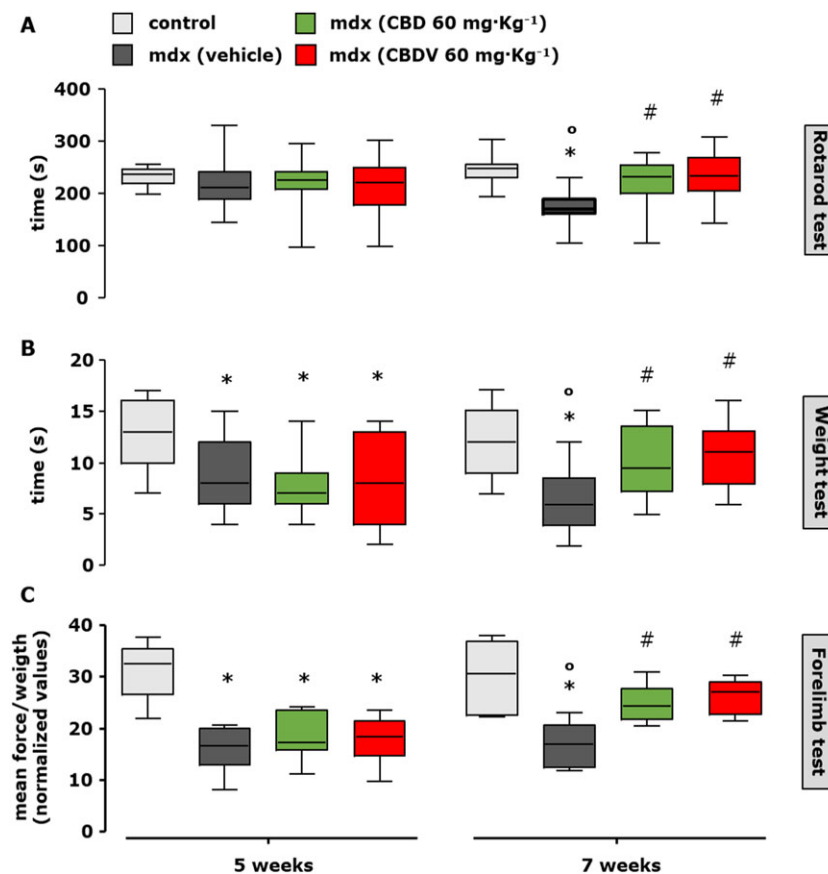


**Figure 7**

Measurement of locomotor activity in control and mdx mice treated or not with CBD or CBDV. Muscle coordination and strength by the rotarod test (A), weight test (B) and (C) forelimb grip strength test were measured in control (C57BL/10ScSn) and dystrophic (C57BL/10ScSn-DMDmdx/J) mice treated with vehicle (10% ethanol + 10% Tween + 80% NaCl; 1:1:8;  $n = 15$ ) or CBD (60 mg·kg<sup>-1</sup>;  $n = 15$ ) or CBDV (60 mg·kg<sup>-1</sup>;  $n = 15$ ) at the beginning of the treatment (5 weeks) and after 2 weeks (7 weeks, right). Control and mdx mice were treated every other day starting from week 5 to week 7 (left). Data sets were compared by one-way ANOVA followed by Bonferroni's test. Differences were considered statistically significant when  $P$  was  $\leq 0.05$ . \*Denotes  $P \leq 0.05$  versus mdx control group at week 5; °  $P \leq 0.05$  versus mdx control group of the same age; #  $P \leq 0.05$  versus mdx vehicle group of the same age.

Tween + NaCl; 1:1:8), there was significant tissue degeneration as compared to control animals of the same age, as shown in the representative images (Figure 8C). The prevalence of centrally positioned nuclei and plausible endomysial fibrosis (Figure 8C, yellow arrows) were clear hallmarks of disease. Treatment with CBD (60 mg·kg<sup>-1</sup>) prevented muscle tissue degeneration (Figure 8C). The effect of CBD on the number of centrally positioned nuclei was quantified and is reported in the bar graphs (Figure 8D).

### *Analysis of regeneration, pro-inflammatory and autophagy markers in skeletal muscle isolated from wild-type and mdx mice exposed to CBD or CBDV*

In order to search for mechanisms through which plant cannabinoids prevented the loss of muscle functionality in mdx mice, we analysed the transcript levels of some of the key genes known to regulate muscle regeneration, inflammation and autophagy in isolated skeletal muscles by qPCR analysis. We found that the gastrocnemius and diaphragm muscles at

7 (Figure 9A,B) and 34 (Figure 9C,D) weeks presented a robust increase in the mRNA expression of the pro-inflammatory markers **IL-6 receptors (IL6R)**, TNF $\alpha$ , **TGF- $\beta$ 1** and **inducible NOS (iNOS)**. A 2 week treatment with either CBD (60 mg·kg<sup>-1</sup>) or CBDV (60 mg·kg<sup>-1</sup>) reduced these transcript levels (Figure 9A–D), but only CBD caused a significant reduction in all transcripts. In order to corroborate these results, we measured by means of ELISA plasma levels of IL-6 and TNF $\alpha$  in control or mdx mice. As expected, plasma levels of both IL-6 and TNF $\alpha$  were considerably increased in mdx mice as compared to wild type. However, CBD- or CBDV-treated mice exhibited a significant reduction in the levels of these two cytokines, comparable to those of control mice of the same age (Figure 9E). Surprisingly, no statistically significant amelioration of the reduced expression of muscle differentiation markers (myogenin, Tnnt-1 and MyHC) was observed after either the 5 to 7 week or 32 to 34 week treatment with either of the two phytocannabinoids (data not shown), suggesting that the effects of CBD and CBDV described here are due more to anti-inflammatory than pro-differentiating actions.

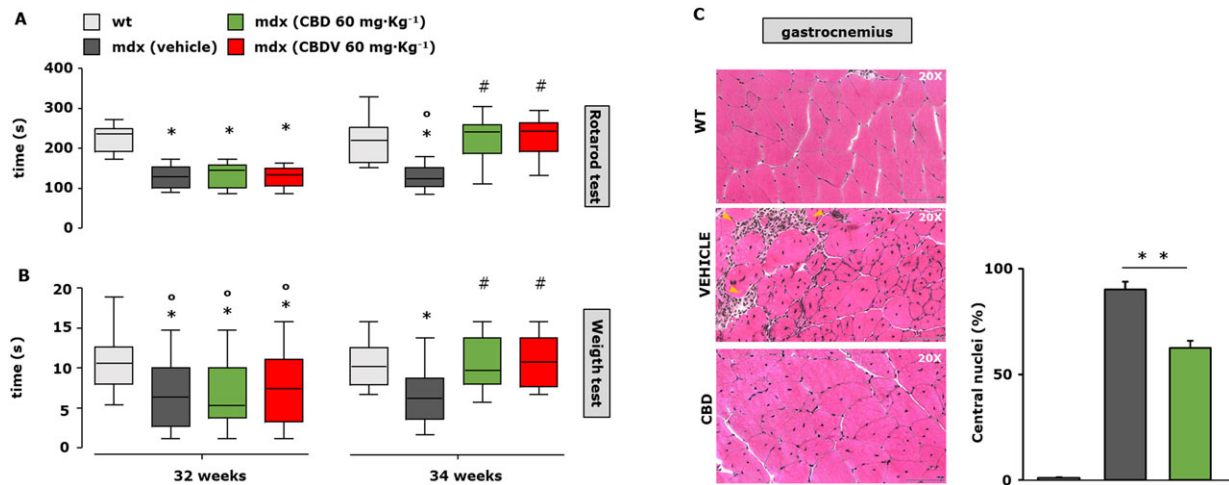


**Figure 8**

Measurement of muscle strength and histological analysis in mdx mice treated with CBD and CBDV. Muscle coordination and strength by the rotarod test (A) and weight test (B) were measured in control (C57BL/10ScSn) and dystrophic (C57BL/10ScSn-DMDmdx/J) mice treated with vehicle (10% ethanol + 10% Tween + 80% NaCl;  $n = 12$ ), CBD (60 mg·kg<sup>-1</sup>;  $n = 12$ ) or CBDV (60 mg·kg<sup>-1</sup>;  $n = 12$ ) at the beginning of the treatment (32 weeks) and after 2 weeks (34 weeks, right). Control and mdx mice were treated every other day starting from week 32 to week 34 (left). Data sets were compared by one-way ANOVA followed by Bonferroni's test. Differences were considered statistically significant when  $P \leq 0.05$ . \*Denotes  $P \leq 0.05$  versus mdx control group at week 5; °  $P \leq 0.05$  versus mdx control group of the same age; #  $P \leq 0.05$  versus mdx vehicle group of the same age. (C) Representative photomicrographs of H&E-stained transverse sections of gastrocnemius muscle isolated from wild type (wt;  $n = 5$ ); mdx treated with vehicle (10% ethanol + 10% Tween + 80% NaCl;  $n = 5$ ) or CBD (60 mg·kg<sup>-1</sup>;  $n = 5$ ) i.p. from week 32 to week 34 of age. Scale bars = 100 µm. (D) The bar graph indicates the number of centralized nuclei in the muscle fibres of control and CBD-treated mdx mice. Data sets were compared by one-way ANOVA followed by Bonferroni's test. \*\* $P \leq 0.001$ .

As mentioned in the introduction, dysregulated autophagy has been implicated in DMD progression (Fiacco *et al.*, 2016). Cannabinoids are not only able to reduce inflammation but also to promote autophagy in various types of cells (Shao *et al.*, 2014; Yang *et al.*, 2014; Costa *et al.*, 2016). Therefore, we evaluated whether the effects of CBD and CBDV at preserving the loss of motor function in mdx mice were attributable to their effect on autophagy. To this purpose, we measured the mRNA expression levels of beclin-1, autophagy-related genes (Atg) 4 and 12, and ULK1, all known markers of autophagy (Terman *et al.*, 2007; Costa *et al.*, 2016), in the gastrocnemius and diaphragm muscles of mdx mice treated with vehicle, CBD or CBDV. As shown in Figure 10A,B, we found that in dystrophic mice of 7 weeks of age, the transcript levels of beclin-1, Atg4, Atg12 and Ulk1 genes were reduced by 60–70% compared to those of age-matched wild-type mice. Importantly, treatment with CBD and CBDV significantly restored the loss of expression of the aforementioned genes, to differing extents, in both types of muscle.

In addition, since autophagosome formation is associated with accumulation of the LC3 II protein, derived from the active cytosolic form LC3-I (Terman *et al.*, 2007), we measured its levels in muscles following exposure to CBD. As shown in the representative western blot (Figure 10C), we found a significant reduction in LC3II expression concomitant with an increase in LC3-I expression, as reported by others (Sandri *et al.*, 2013; Fiacco *et al.*, 2016). Treatment with CBD promoted the formation of LC3II ( $F_{(5, 24)} = 48.71$ ,  $P < 0.05$ ) at the expense of LC3-I ( $F_{(5, 24)} = 48.71$ ,  $P < 0.05$ ), which is associated with the promotion of autophagy. Figure 10D shows the quantification of these results.

## Discussion

We present evidence in favour of the possible use of some non-euphoric phytocannabinoids to ameliorate certain pathological aspects of DMD. Unlike THC, the cannabinoids investigated here are devoid of agonist activity at cannabinoid CB<sub>1</sub> receptors, a very abundant GPCR in the mammalian brain, responsible for most of the euphoric effects of marijuana (Iannotti *et al.*, 2016). CBD is being currently developed for the treatment of seizures in genetic paediatric epilepsies resistant to conventional anticonvulsant agents (Slomski, 2017), has been shown to be a safe alternative to an antipsychotic for the treatment of schizophrenia (Rohleder *et al.*, 2016) and is useful in a plethora of central and peripheral disorders in animal models (McPartland *et al.*, 2015). CBDV is being assessed as an anti-convulsant (Hill *et al.*, 2012), whereas THCV has been tested against dyslipidaemia and glucose intolerance in two phase II clinical trials (Jadoon *et al.*, 2016). In view of the efficacy and safety of CBD, CBDV and THCV in clinical trials and of the fact that CB<sub>1</sub> receptor activation with potential euphoric actions was reported to worsen muscle differentiation and stimulate myoblast proliferation and to have a negative effect on muscle formation (Iannotti *et al.*, 2014b), we decided to investigate these three compounds on myoblast differentiation. Our data suggest that (i) CBD and CBDV stimulate the differentiation of murine myoblasts and human DMD myoblasts into myotubes; (ii) CBD, CBDV and THCV stimulate the differentiation into myotubes of human muscle satellite cells; and (iii) CBD and CBDV ameliorate impaired locomotor activity and muscle strength in mdx mice at both the early and late

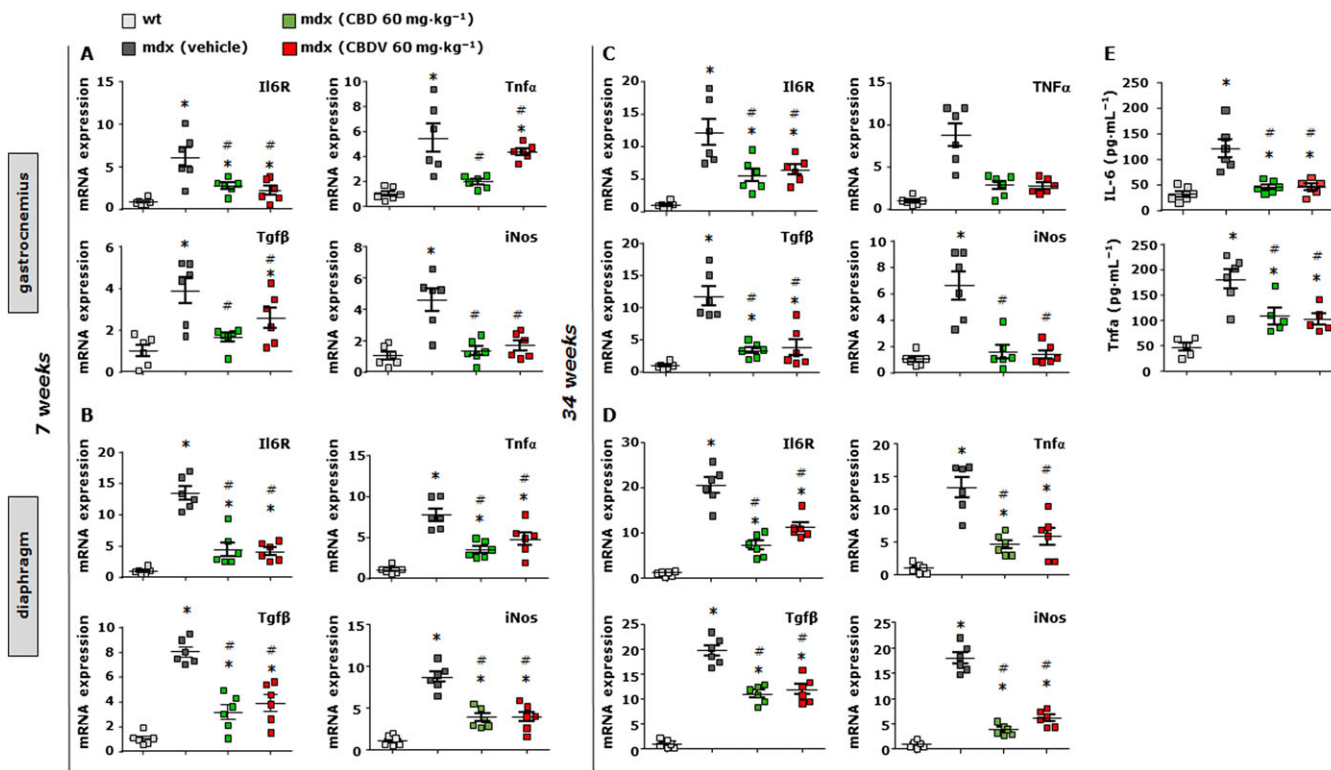


**Figure 9**

Analysis of expression of inflammation markers in skeletal muscles of mdx mice treated with CBD and CBDV. Scatter plot graphs showing the mRNA expression levels of IL-6 receptors (IL6R), TNF $\alpha$ , TGF- $\beta$ 1 and iNOS in the gastrocnemius and/or diaphragm muscles of control and mdx mice of both 7 (A and B) and 34 (C and D) weeks of age that had received vehicle or CBD or CBDV for 2 weeks. Data are expressed as  $2^{-\Delta\Delta Ct}$  relative to S16, as described in Methods. (E) plasma levels of IL-6 and TNF $\alpha$  quantified by ELISA assay in control and mdx mice (34 weeks) treated with vehicle, CBD or CBDV. Data represent the mean  $\pm$  SEM of  $\geq 5$  independent determinations. Data sets were compared by one-way ANOVA followed by Bonferroni's test. \*Denotes  $P \leq 0.05$  versus mdx control group at week 5; # $P \leq 0.05$  versus mdx vehicle group of the same age.

stages of the disorder, this effect being accompanied by a significant reduction in markers of inflammation and a restoration of markers of autophagy.

In murine C2C12 myoblasts, the pro-differentiating effects of CBD and CBDV were identified by quantifying the expression of two typical marker genes of muscle differentiation and were confirmed by morphological analyses, indicating cell fusion and formation of multi-nucleated myotubes. These effects were as follows: (i) strongest with short incubation times of myoblasts with CBD and CBDV; (ii) mimicked by a TRPV1 agonist and counteracted by a TRPV1 antagonist; and (iii) accompanied by an elevation of  $[Ca^{2+}]_i$ , a response mimicked by a TRPV1 agonist and counteracted by a TRPV1 antagonist. These observations indicate that the pro-differentiating effects of CBD and CBDV in C2C12 cells are due to activation of TRPV1 channels and, possibly, subsequent elevation of  $[Ca^{2+}]_i$ , pointing to this channel as an important player in murine myoblast-to-myotube differentiation (Kurosaka *et al.*, 2016). The concentration–response curves obtained following the stimulation with CBD and/or CBDV indicate complex actions on the target or involvement of multiple targets. Interestingly, Ito *et al.* (2013) demonstrated that in isolated muscle fibres, capsaicin induces an increase in intracellular calcium levels in a TRPV1-dependent

manner, an effect that they suggested as a possible cause of muscle hypertrophy.

Importantly, CBD and CBDV significantly increased the expression of differentiation markers in myoblasts from DMD donors. It would be interesting, in future studies employing a more statistically relevant number of donor samples, to look for correlations between the occurrence of given mutations and responsiveness to phytocannabinoids. In view of our results in human satellite cells (see below), future experiments will need to address the question of what molecular target(s) is/are involved in the pro-differentiating effects of CBD and CBDV in human myoblasts.

Skeletal muscle satellite cells play a crucial role in muscle regeneration, for example, following damage or physical exercise. DMD also affects the capability of these cells to differentiate into myotubes (Chang *et al.*, 2016). Using human satellite cells, we showed that CBD and CBDV, but also THCV, are capable of enhancing differentiation, thus potentially extending the therapeutic usefulness of these compounds at counteracting dystrophies. Interestingly, the target through which these compounds produce their differentiating effect appears to be different from that mediating this effect in murine C2C12 myoblasts. In fact, TRPA1, rather than TRPV1, channels mediated both these effects, and the

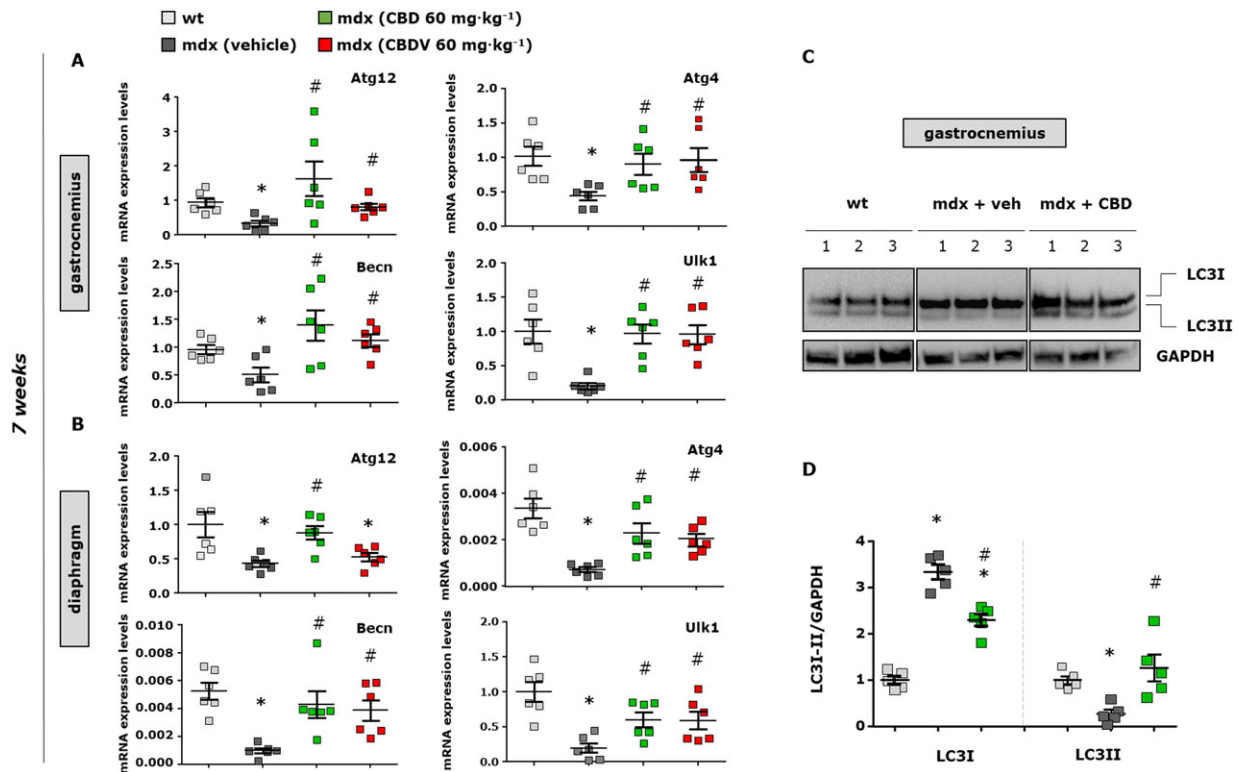


**Figure 10**

Expression analysis of autophagy markers in skeletal muscles of mdx mice treated with CBD and CBDV. The scatter plot graphs show the mRNA expression levels of autophagy-related 12 and 4b (ATG12 or 4b), beclin-1 (becn1) and ULK1 genes in the gastrocnemius (A) and/or diaphragm (B) muscles of control and dystrophic mdx mice of 7 weeks that received vehicle or CBD or CBDV for the last 2 weeks. Data are expressed as  $2^{-\Delta\Delta Ct}$  relative to S16, as described in Methods. (C) Representative blot showing the band intensity of the autophagic marker LC3I/II in the gastrocnemius muscles of mdx mice treated with CBD. (D) Bar graph showing the quantification of LC3I/II levels normalized to GAPDH. Data represent the mean  $\pm$  SEM of  $\geq 5$  separate determinations. Data sets were compared by one-way ANOVA followed by Bonferroni's test. Differences were considered statistically significant when  $P \leq 0.05$ . \*Denotes  $P \leq 0.05$  versus mdx control group at week 5; # $P \leq 0.05$  versus mdx vehicle group of the same age.

elevation of  $[Ca^{2+}]_i$ . TRPA1 in satellite cells also undergoes down-regulation following differentiation into myotubes, thus providing a negative feedback mechanism for this process. Future experiments will need to investigate the role of TRPA1 in satellite cell differentiation.

The finding that CBD and CBDV promote both murine myoblast and human satellite cell differentiation prompted the testing of these compounds on muscle function in mdx mice. Indeed, a 2 week treatment of dystrophic mice with either phytocannabinoid lead to amelioration of their locomotor activity, evaluated with the rotarod test, and muscle strength was assessed with the weight and forelimb grip strength test. Importantly, such an amelioration was seen both when treatment was given when the signs of the disorder were just appearing and, at a late stage, when such signs were stronger. Intriguingly, however, with both types of treatment, we could not confirm *ex vivo* the pro-differentiating effects of CBD and CBDV observed *in vitro*, thus raising the possibility that the effects observed were due to an action other than enhancement of myotube formation. Indeed, DMD is a complex pathology that rapidly evolves in several directions through subsequent maladaptive and vicious circle-generating mechanisms, encompassing, among others,

chronic inflammation, fibrosis and defective autophagy (Fiacco *et al.*, 2016). Therefore, we investigated if, at the end of treatment, the beneficial effects of the phytocannabinoids were accompanied by local or systemic anti-inflammatory effects or by the restoration of autophagy. The analysis of transcripts, which were pathologically altered in untreated mdx muscles, suggested that CBD and CBDV reduced the consequences of inflammation and impaired autophagy, thus possibly explaining their effects. Since we did not perform a detailed time course experiment on all these biomarkers, we cannot draw any conclusion as to whether the anti-inflammatory effects of the phytocannabinoids are the cause or the consequence of their pro-autophagic actions or whether at different stages of the disease, these compounds may affect myoblast differentiation. However, these anti-inflammatory and pro-autophagic actions open the possibility of testing CBD and CBDV as add-on therapeutics to other agents that are currently undergoing clinical trials in DMD, such as exon-skipping agents (Nakamura, 2017). It is worth mentioning that mdx mice do not represent an archetypal model of all aspects of the human DMD disease. Therefore, whilst beyond the scope of the present investigation, future studies in more suitable models, such as the golden retriever

dog (Collins and Morgan, 2003; McGreevy *et al.*, 2015), are needed in order to investigate the therapeutic utility of CBD and CBDV in DMD.

In conclusion, we report for the first time the potential for some non-euphoric phytocannabinoids to potentially counteract at least three of the pathological features of DMD, that is, impaired myoblast and satellite cell differentiation, unresolved inflammation and defective autophagy. These findings should encourage studies in more suitable animal models of DMD with the aim of specifically assessing the clinical potential of CBD and CBDV as add-on therapies against this type or other types of muscular dystrophies.

## Acknowledgements

This research was supported by GW Pharmaceuticals, Cambridge, UK. We thank Prof. Ben Whalley and Dr Will Hind (GW Pharmaceuticals) for critical reading of the manuscript.

## Author contributions

F.A.I., V.D., E.P., R.C. and E.D. contributed to the design and concept of the study. F.A.I., E.P., R.C., A.S.M., L.D., E.G., F.A., N.C.S. and L.D. performed the experiments. F.A.I., E.P., R.C., N.C.S. and V.D. analysed and interpreted the data. F.A.I. and V.D. wrote the manuscript.

## Conflicts of interest

F.A.I. and V.D. are supported by GW Pharmaceuticals, UK, for research on phytocannabinoids and skeletal muscle degenerative disorders (grant number GWCRI15107 to F.A.I.). V.D. has a Consultancy Agreement with GW Pharmaceuticals.

## Declaration of transparency and scientific rigour

This Declaration acknowledges that this paper adheres to the principles for transparent reporting and scientific rigour of preclinical research recommended by funding agencies, publishers and other organisations engaged with supporting research.

## References

Alexander SPH, Christopoulos A, Davenport AP, Kelly E, Marrion NV, Peters JA *et al.* (2017a). The Concise Guide to PHARMACOLOGY 2017/18: G protein-coupled receptors. *Br J Pharmacol* 174: S17–S129.

Alexander SPH, Fabbro D, Kelly E, Marrion NV, Peters JA, Faccenda E *et al.* (2017b). The Concise Guide to PHARMACOLOGY 2017/18: Catalytic receptors. *Br J Pharmacol* 174: S225–S271.

Alexander SPH, Fabbro D, Kelly E, Marrion NV, Peters JA, Faccenda E *et al.* (2017c). The Concise Guide to PHARMACOLOGY 2017/18: Enzymes. *Br J Pharmacol* 174: S272–S359.

Alexander SP, Striessnig J, Kelly E, Marrion NV, Peters JA, Faccenda E *et al.* (2017d). The Concise Guide to PHARMACOLOGY 2017/18: Voltage-gated ion channels. *Br J Pharmacol* 174: S160–S194.

Aartsma-Rus A, van Putten M (2014). Assessing functional performance in the mdx mouse model. *J Vis Exp* 85: S1303.

Burstein SH, Zurier RB (2009). Cannabinoids, endocannabinoids, and related analogues in inflammation. *AAPS J* 11: 109–119.

Chang NC, Chevalier FP, Rudnicki MA (2016). Satellite cells in muscular dystrophy – lost in polarity. *Trends Mol Med* 22: 479–496.

Collins CA, Morgan JE (2003). Duchenne's muscular dystrophy: animal models used to investigate pathogenesis and develop therapeutic strategies. *Int J Exp Pathol* 84: 165–172.

Cooper E (2001). A new role for ion channels in myoblast fusion. *J Cell Biol* 153: f9–f12.

Cortright DN, Szallasi A (2004). Biochemical pharmacology of the vanilloid receptor TRPV1. An update. *Eur J Biochem* 271: 1814–1819.

Costa L, Amaral C, Teixeira N, Correia-da-Silva G, Fonseca BM (2016). Cannabinoid-induced autophagy: protective or death role? *Prostaglandins Other Lipid Mediat* 122: 54–63.

Cruz-Guzmán OR, Rodríguez-Cruz M, Escobar Cedillo RE (2015). Systemic inflammation in Duchenne muscular dystrophy: association with muscle function and nutritional status. *Biomed Res Int* 2015: 891972.

Curtis MJ, Alexander S, Cirino G, Docherty JR, George CH, Giembycz MA *et al.* (2018). Experimental design and analysis and their reporting II: updated and simplified guidance for authors and peer reviewers. *Br J Pharmacol* 175: 987–993.

De Palma C, Perrotta C, Pellegrino P, Clementi E, Cervia D (2014). Skeletal muscle homeostasis in duchenne muscular dystrophy: modulating autophagy as a promising therapeutic strategy. *Front Aging Neurosci* 6: 188.

De Petrocellis L, Guida F, Moriello AS, De Chiaro M, Piscitelli F, de Novellis V *et al.* (2011a). N-palmitoyl-vanillamide (palvanil) is a non-pungent analogue of capsaicin with stronger desensitizing capability against the TRPV1 receptor and anti-hyperalgesic activity. *Pharmacol Res* 63: 294–299.

De Petrocellis L, Ligresti A, Moriello AS, Allarà M, Bisogno T, Petrosino S *et al.* (2011b). Effects of cannabinoids and cannabinoid-enriched Cannabis extracts on TRP channels and endocannabinoid metabolic enzymes. *Br J Pharmacol* 163: 1479–1494.

Deacon RM (2013). Measuring the strength of mice. *J Vis Exp* (76): 2610.

Di Marzo V, De Petrocellis L (2010). Endocannabinoids as regulators of transient receptor potential (TRP) channels: a further opportunity to develop new endocannabinoid-based therapeutic drugs. *Curr Med Chem* 17: 1430–1449.

Di Marzo V, Piscitelli F (2015). The endocannabinoid system and its modulation by phytocannabinoids. *Neurotherapeutics* 12: 692–698.

Duddy W, Duguez S, Johnston H, Cohen TV, Phadke A, Gordish-Dressman H *et al.* (2015). Muscular dystrophy in the mdx mouse is a severe myopathy compounded by hypotrophy, hypertrophy and hyperplasia. *Skelet Muscle* 5: 16.

Dumont NA, Wang YX, von Maltzahn J, Pasut A, Bentzinger CF, Brun CE *et al.* (2015). Dystrophin expression in muscle stem cells regulates their polarity and asymmetric division. *Nat Med* 21: 1455–1463.

Fernández-Ruiz J, Sagredo O, Pazos MR, García C, Pertwee R, Mechoulam R *et al.* (2013). Cannabidiol for neurodegenerative

disorders: important new clinical applications for this phytocannabinoid? *Br J Clin Pharmacol* 75: 323–333.

Fiacco E, Castagnetti F, Bianconi V, Madaro L, De Bardi M, Nazio F *et al.* (2016). Autophagy regulates satellite cell ability to regenerate normal and dystrophic muscles. *Cell Death Differ* 23: 1839–1849.

Fischedick JT (2017). Identification of terpenoid chemotypes among high (–)-trans- $\Delta^9$ -tetrahydrocannabinol-producing *Cannabis sativa* L. Cultivars. *Cannabis Cannabinoid Res* 2: 34–47.

Gailly P (2012). TRP channels in normal and dystrophic skeletal muscle. *Curr Opin Pharmacol* 12: 326–334.

Govoni A, Magri F, Brajkovic S, Zanetta C, Faravelli I, Corti S *et al.* (2013). Ongoing therapeutic trials and outcome measures for Duchenne muscular dystrophy. *Cell Mol Life Sci* 70: 4585–4602.

Harding SD, Sharman JL, Faccenda E, Southan C, Pawson AJ, Ireland S *et al.* (2018). The IUPHAR/BPS Guide to PHARMACOLOGY in 2018: updates and expansion to encompass the new guide to IMMUNOPHARMACOLOGY. *Nucl Acids Res* 46: D1091–D1106.

Hassan S, Eldeeb K, Millns PJ, Bennett AJ, Alexander SP, Kendall DA (2014). Cannabidiol enhances microglial phagocytosis via transient receptor potential (TRP) channel activation. *Br J Pharmacol* 171: 2426–2439.

Hill AJ, Mercier MS, Hill TD, Glyn SE, Jones NA, Yamasaki Y *et al.* (2012). Cannabidiol is anticonvulsant in mouse and rat. *Br J Pharmacol* 167: 1629–1642.

Iannotti FA, Di Marzo V, Petrosino S (2016). Endocannabinoids and endocannabinoid-related mediators: Targets, metabolism and role in neurological disorders. *Prog Lipid Res* 62: 107–128.

Iannotti FA, Hill CL, Leo A, Alhusaini A, Soubrane C, Mazzarella E *et al.* (2014a). Non-psychoactive plant cannabinoids, cannabidiol (CBDV) and cannabidiol (CBD), activate and desensitize transient receptor potential vanilloid 1 (TRPV1) channels *in vitro*: potential for the treatment of neuronal hyperexcitability. *ACS Chem Neurosci* 5: 1131–1141.

Iannotti FA, Panza E, Barrese V, Viggiano D, Soldovieri MV, Tagliatela M (2010). Expression, localization, and pharmacological role of Kv7 potassium channels in skeletal muscle proliferation, differentiation, and survival after myotoxic insults. *J Pharmacol Exp Ther* 332: 811–820.

Iannotti FA, Silvestri C, Mazzarella E, Martella A, Calvigioni D, Piscitelli F *et al.* (2014b). The endocannabinoid 2-AG controls skeletal muscle cell differentiation via CB1 receptor-dependent inhibition of Kv7 channels. *Proc Natl Acad Sci U S A* 111: E2472–E2481.

Iffland K, Grotenhermen F (2017). An update on safety and side effects of cannabidiol: a review of clinical data and relevant animal studies. *Cannabis Cannabinoid Res* 2: 139–154.

Ito N, Ruegg UT, Kudo A, Miyagoe-Suzuki Y, Takeda S (2013). Activation of calcium signaling through TRPV1 by nNOS and peroxynitrite as a key trigger of skeletal muscle hypertrophy. *Nat Med* 19: 101–106.

Iwata Y, Ohtake H, Suzuki O, Matsuda J, Komamura K, Wakabayashi S (2013). Blockade of sarcolemmal TRPV2 accumulation inhibits progression of dilated cardiomyopathy. *Cardiovasc Res* 99: 760–768.

Jadoon KA, Ratcliffe SH, Barrett DA, Thomas EL, Stott C, Bell JD *et al.* (2016). Efficacy and safety of cannabidiol and tetrahydrocannabinol on glycemic and lipid parameters in patients with type 2 diabetes: a randomized, double-blind, placebo-controlled, parallel group pilot study. *Diabetes Care* 39: 1777–1786.

Jendryke T, Prochazkova M, Hall BE, Nordmann GC, Schladt M, Milenkovic VM *et al.* (2016). TRPV1 function is modulated by Cdk5-mediated phosphorylation: insights into the molecular mechanism of nociception. *Sci Rep* 6: 22007.

Kilkenny C, Browne W, Cuthill IC, Emerson M, Altman DG (2010). Animal research: reporting *in vivo* experiments: the ARRIVE guidelines. *Br J Pharmacol* 160: 1577–1579.

Kurosaka M, Ogura Y, Funabashi T, Akema T (2016). Involvement of transient receptor potential cation channel vanilloid 1 (TRPV1) in myoblast fusion. *J Cell Physiol* 231: 2275–2285.

Lorin C, Vögeli I, Niggli E (2015). Dystrophic cardiomyopathy: role of TRPV2 channels in stretch-induced cell damage. *Cardiovasc Res* 106: 153–162.

Magri F, Govoni A, D'Angelo MG, Del Bo R, Ghezzi S, Sandra G *et al.* (2011). Genotype and phenotype characterization in a large dystrophinopathic cohort with extended follow-up. *J Neurol* 258: 1610–1623.

Matsumura K, Ohlendieck K, Ionasescu VV, Tomé FM, Nonaka I, Burghes AH *et al.* (1993). The role of the dystrophin-glycoprotein complex in the molecular pathogenesis of muscular dystrophies. *Neuromuscul Disord* 3: 533–535.

McGrath JC, Lilley E (2015). Implementing guidelines on reporting research using animals (ARRIVE etc.): new requirements for publication in BJP. *Br J Pharmacol* 172: 3189–3193.

McGreevy JW, Hakim CH, McIntosh MA, Duan D (2015). Animal models of Duchenne muscular dystrophy: from basic mechanisms to gene therapy. *Dis Model Mech* 8: 195–213.

McPartland JM, Duncan M, Di Marzo V, Pertwee RG (2015). Are cannabidiol and  $\Delta^9$ -tetrahydrocannabinol negative modulators of the endocannabinoid system? A systematic review. *Br J Pharmacol* 172: 737–753.

Miyatake S, Shimizu-Motohashi Y, Takeda S, Aoki Y (2016). Anti-inflammatory drugs for Duchenne muscular dystrophy: focus on skeletal muscle-releasing factors. *Drug Des Devel Ther* 10: 2745–2758.

Mohapatra DP, Nau C (2005). Regulation of  $Ca^{2+}$ -dependent desensitization in the vanilloid receptor TRPV1 by calcineurin and cAMP-dependent protein kinase. *J Biol Chem* 280: 13424–13432.

Morales P, Hurst D, Reggio P (2017). Molecular targets of the phytocannabinoids: a complex picture. *Prog Chem Org Nat Prod* 103: 103–131.

Morosetti R, Broccolini A, Sancricca C, Gliubizzi C, Gidaro T, Tonali PA *et al.* (2010). Increased aging in primary muscle cultures of sporadic inclusion-body myositis. *Neurobiol Aging* 31: 1205–1214.

Nakamura A (2017). Moving towards successful exon-skipping therapy for Duchenne muscular dystrophy. *J Hum Genet* 62: 871–876.

Nie L, Oishi Y, Doi I, Shibata H, Kojima I (1997). Inhibition of proliferation of MCF-7 breast cancer cells by a blocker of  $Ca^{2+}$ -permeable channel. *Cell Calcium* 22: 75–82.

Okubo K, Matsumura M, Kawaiishi Y, Aoki Y, Matsunami M, Okawa Y *et al.* (2012). Hydrogen sulfide-induced mechanical hyperalgesia and allodynia require activation of both Cav3.2 and TRPA1 channels in mice. *Br J Pharmacol* 166: 1738–1743.

Pan Z, Zhao X, Brotto M (2012). Fluorescence-based measurement of store-operated calcium entry in live cells: from cultured cancer cell to skeletal muscle fiber. *J Vis Exp* 60: pii: 3415.



- Patel A, Hirst RA, Harrison C, Hirota K, Lambert DG (2013). Measurement of  $[Ca^{2+}]_i$  in whole cell suspensions using Fura-2. *Methods Mol Biol* 937: 37–47.
- Robbins N, Koch SE, Tranter M, Rubinstein J (2012). The history and future of probenecid. *Cardiovasc Toxicol* 12: 1–9.
- Robinson JA, Jenkins NS, Holman NA, Roberts-Thomson SJ, Monteith GR (2004). Ratiometric and nonratiometric  $Ca^{2+}$  indicators for the assessment of intracellular free  $Ca^{2+}$  in a breast cancer cell line using a fluorescence microplate reader. *J Biochem Biophys Methods* 58: 227–237.
- Rohleder C, Müller JK, Lange B, Leweke FM (2016). Cannabidiol as a potential new type of an antipsychotic. A critical review of the evidence. *Front Pharmacol* 7: 422.
- Sandri M, Coletto L, Grumati P, Bonaldo P (2013). Misregulation of autophagy and protein degradation systems in myopathies and muscular dystrophies. *J Cell Sci* 126 (Pt 23): 5325–5333.
- Seabrook GR, Sutton KG, Jarolimek W, Hollingworth GJ, Teague S, Webb J *et al.* (2002). Functional properties of the high-affinity TRPV1 (VR1) vanilloid receptor antagonist (4-hydroxy-5-iodo-3-methoxyphenylacetate ester) iodo-resiniferatoxin. *J Pharmacol Exp Ther* 303: 1052–1060.
- Shao BZ, Wei W, Ke P, Xu ZQ, Zhou JX, Liu C (2014). Activating cannabinoid receptor 2 alleviates pathogenesis of experimental autoimmune encephalomyelitis via activation of autophagy and inhibiting NLRP3 inflammasome. *CNS Neurosci Ther* 20: 1021–1028.
- Slomski A (2017). Fewer seizures with cannabidiol in catastrophic epilepsy. *JAMA* 318: 323.
- Terman A, Gustafsson B, Brunk UT (2007). Autophagy, organelles and ageing. *J Pathol* 211: 134–143.
- Vyklický L, Nováková-Tousová K, Benedikt J, Samad A, Touska F, Vlachová V (2008). Calcium-dependent desensitization of vanilloid receptor TRPV1: a mechanism possibly involved in analgesia induced by topical application of capsaicin. *Physiol Res* 57 (Suppl. 3): S59–S68.
- Yang L, Rozenfeld R, Wu D, Devi LA, Zhang Z, Cederbaum A (2014). Cannabidiol protects liver from binge alcohol-induced steatosis by mechanisms including inhibition of oxidative stress and increase in autophagy. *Free Radic Biol Med* 68: 260–267.
- Zurier RB, Burstein SH (2016). Cannabinoids, inflammation, and fibrosis. *FASEB J* 30: 3682–3689.

## Supporting Information

Additional supporting information may be found online in the Supporting Information section at the end of the article.

<https://doi.org/10.1111/bph.14460>

**Figure S1** Measurement of skeletal muscle differentiation markers in C2C12 cells upon exposure to CBD, CBDV, THCV, CBG and CBDA. Transcript levels of myogenin (Myog) in murine C2C12 cells exposed to differentiation media DM in presence of crescent concentration (from 0.1 to 3  $\mu$ M) of CBD (A), CBDV (B), THCV (C), CBG (D) or CBDA (E) for 72 h. The quantification of transcripts for Myog and Tnnt-T1 was performed by quantitative real-time PCR. Data are expressed as  $2^{-\Delta\Delta ct}$  relative to S16, as described in materials and methods. Data represent the mean  $\pm$  S.E.M. of 5 separate determinations. Data sets were compared by one-way ANOVA followed by Bonferroni's test. Differences were considered statistically significant when  $P$  was  $\leq 0.05$ .

**Figure S2** Effect of TRPV1 and TRPV2 agonists or antagonists in differentiating C2C12 cells. Transcript levels of Myogenin (Myog) and troponin T1 (Tnnt-T1) in murine C2C12 cells exposed to differentiation media DM for 72 h in presence of increasing concentration of palvanil (A), IRTX (B), probenecid (C) or tranilast (D). The quantification of transcripts for Myog and Tnnt-T1 was performed by quantitative real-time PCR. Data are expressed as  $2^{-\Delta\Delta ct}$  relative to S16, as described in materials and methods. Data represent the mean  $\pm$  S.E.M. of  $\geq 5$  separate determinations. Data sets were compared by use of one-way ANOVA followed by Bonferroni's test. Differences were considered statistically significant when  $P$  was  $\leq 0.05$ .

**Figure S3** Evaluation of TRPV1 phosphorylation in C2C12 cells upon exposure to palvanil. Representative blot showing the TRPV1 protein expression and changes in its phosphorylation at S800 evaluated through western blot analysis in C2C12 cells exposed for 72 h to palvanil 0.3  $\mu$ M or IRTX 1  $\mu$ M. (B) Bar graph showing the quantification of pTRPV1 levels normalized to total TRPV1. Data represent the mean  $\pm$  S.E.M. of 5 separate determinations. Data sets were compared by use of one-way ANOVA followed by Bonferroni's test.

**Figure S4** Effect of CBDV and THCV in TRPA1 silenced satellite cells (A) The graph shows the quantification of intracellular  $Ca^{2+}$  levels upon exposure to CBDV or THCV (3  $\mu$ M) of human satellite cells transiently transfected with scramble or TRPA1 siRNA. (B) Effect of CBDV and THCV 3  $\mu$ M on MYOG expression in differentiating TRPA1-silenced satellite cells. Data represent the mean  $\pm$  S.E.M. of 5 separate determinations. Data sets were compared by one-way ANOVA followed by Bonferroni's test. Differences were considered statistically significant when  $P$  was  $\leq 0.05$ .

**Table S1** TRP channel expression levels in murine C2C12 (A) and human satellite cells (B).

**Table S2** Clinical indices of DMD patients.

**Table S3** List of primers used in qPCR analysis.